

AN ABSTRACT OF THE THESIS OF

RANDALL JAY CHARBENEAU for the degree of MASTER OF SCIENCE

in CIVIL ENGINEERING presented on May 27, 1975

Title: AMBIENT CURRENT EFFECTS ON VERTICAL SELECTIVE FLOW

WITHDRAWAL IN A TWO LAYER RESERVOIR SYSTEM

Redacted for privacy

Abstract approved:

 Larry S. Slotta

Withdrawal from a two-layer flow field is examined in terms of the degree of selectivity of the withdrawal flow and its dependence on an ambient current. Selectivity is defined as the bias of withdrawing one layer more strongly than the other; the extreme case is complete selective withdrawal, where one layer is drawn in alone. Relevant physical parameters included in the study are: the rate of withdrawal, dimensions of the intake, the depth of each layer, and the elevation of the intake above the two strata density-interface. The fluid parameters of interest are density and viscosity. Significant flow phenomena include: the limiting conditions of selective withdrawal, stability of the interface, interfacial waves, velocity shear and mass transport.

Withdrawal from a two strata flow field to a point sink located in the upper strata is examined experimentally. Tests are made for various density differentials across the interface, elevations between the intake and the interface, and relative velocities between the flow

field and the intake. The results show that within a range of separating heights of the intake from the interface the degree of selectivity is a quasi-linear function of the separating height. Of special interest is the observation that the degree of selectivity approaches unity slowly after passing a critical value of the dimensionless separation height. The influence of the density difference across the interfacial region is negligible when the intake is close to the density-interface, but increases in importance as the separating height is increased.

For selective stratified flow withdrawal the influence of ambient currents is complex. Generation of interfacial waves caused by the moving intake (which acts as a moving low-pressure area) can both increase and decrease the selective withdrawal. If such waves can be excluded then an ambient current would be expected to enhance the phenomena of selective withdrawal.

Ambient Current Effects on Vertical Selective Flow  
Withdrawal in a Two Layer Reservoir System

by

Randall Jay Charbeneau

A THESIS

submitted to

Oregon State University


in partial fulfillment of  
the requirements for the  
degree of

Master of Science

June 1976

APPROVED:

Redacted for privacy

 Professor of Civil Engineering \_\_\_\_\_

in charge of major

Redacted for privacy

Head of Department of Civil Engineering \_\_\_\_\_

Redacted for privacy

Dean of Graduate School \_\_\_\_\_

Date thesis is presented May 27, 1975

## ACKNOWLEDGMENT

The author is grateful to the individuals that have aided in this experimental study. Special thanks is given for the advice and continued encouragement and interest of Dr. Larry S. Slotta who served as major professor. Thanks is also given to Dr. Gerritt Abraham for his valuable suggestions early in the work. Financial support for the work was provided by the United States Department of the Interior, Office of Water Research and Technology, as authorized under the Water Resources Research Act of 1964, P. L. 88-379. During the period of thesis preparation the author received support from the Departments of Agricultural Engineering and Civil Engineering, which was truly appreciated. Most of all, the author is grateful for the encouragement and patience of Nancy.

## TABLE OF CONTENTS

	Page
INTRODUCTION	1
Selective Withdrawal - General	1
Degree of Selectivity	4
Densimetric Froude Number	6
Literature Review	8
Problem Formulation	16
EXPERIMENT	21
Laboratory Equipment	21
Procedure	25
Methods of Observation - Analysis	28
FLOW PHENOMENA	30
Interfacial Shear and Associated Density Transport	30
Interfacial Waves	32
Creation of Waves by a Moving Disturbance	33
Capillarity	36
EXPERIMENTAL RESULTS AND DISCUSSION	39
Influence of the Proximity and Density Differential Parameters	39
Influence of an Ambient Current	59
Significance for Thermocline Structure	69
CONCLUSIONS	72
BIBLIOGRAPHY	74
APPENDIX	76

## LIST OF FIGURES

Figure		Page
1	Experimental design	2
2	Critical fully-selective withdrawal conditions	10
3	Configuration discussed by Williams (22)	17
4	Experimental set-up	23
5	Plexiglass standpipe design	24
6	Position of generated wave (from Wiegel, <u>et al.</u> 1958)	37
7	Relation of the degree of selectivity to the separating height	42
8	Relation of the degree of selectivity to the proximity parameter	44
9	Relation of the degree of selectivity to the proximity parameter having range less than unity	45
10	Influence of the density differential on the degree of selectivity; proximity parameter less than unity	47
11	Typical withdrawal cones: $\frac{\Delta\rho}{\rho_1} = 0.081, u = 0$	49
12	Relation of the proximity parameter to the intake diameter parameter	51
13	Relation of the degree of selectivity to the cross-sectional area parameter	52
14	Relation of the radial velocity to the radial distance from the intake	56
15	Influence of the density differential on the degree of selectivity; proximity parameter greater than unity	57
16	Iso-selectivity curves	58
17	Typical locations and shapes of withdrawal cones	62
18	Relation of the relative selectivity to the ambient velocity	64

Figure		Page
19	Relation of the relative selectivity to the ambient velocity; $\frac{\Delta\rho}{\rho_1} = 0.022$	66
20	Relation of the choking coefficient to the proximity parameter	70



## LIST OF PLATES

Plate		Page
1	Typical withdrawal cone: $\frac{z}{z_c} = 0.71$ , $\frac{\Delta\rho}{\rho_1} = 0.081$ , $u = 0$	50
2	Shear withdrawal from the lower layer: $\frac{z}{z_c} = 1.19$ , $\frac{\Delta\rho}{\rho_1} = 0.022$ , $u = 0$ , $S_1 = \frac{Q_1}{Q_t} = 0.96$	54
3-6	Capillary entrainment sequence where $u = 10.3$ cm/sec.	68

## LIST OF SYMBOLS

$A_i$	intake cross-sectional area
$A_c^*$	cross-sectional area of the withdrawal cone from the lower layer at the jet vena contracta
$c$	wave celerity
$D$	intake diameter (cm.)
$D_c$	diameter of the withdrawal cone from the lower layer
$D_c^*$	diameter of the withdrawal cone at the jet vena contracta
$g$	gravitational acceleration
$h_i$	depth of the $i^{\text{th}}$ layer (cm.)
$Q$	discharge (cc/sec.)
$Q_t$	total discharge through the intake
$S_i$	degree of selectivity; referenced to the $i^{\text{th}}$ layer ( $= \frac{Q_i}{Q_t}$ )
$V_c$	intake velocity (cm/sec.)
$V_c$	critical intake velocity
$V_1, V_2$	velocities of the upper and lower layers, measured across the interfacial region
$z$	intake-interface separation height (cm.)
$z_0, z_c$	critical intake-interface separation height
$\rho$	fluid density (gm/cc.)
$\rho_i$	fluid density of the $i^{\text{th}}$ layer
$\Delta\rho$	change in density measured across the interfacial region

AMBIENT CURRENT EFFECTS ON VERTICAL SELECTIVE FLOW  
WITHDRAWAL IN A TWO LAYER RESERVOIR SYSTEM

I. INTRODUCTION

This study examined the way in which selectivity of flow withdrawal into a vertically suspended upper strata point sink is affected by an ambient current in a two-layer system. The goals were

1. to determine whether the presence of an ambient current inhibits the possibility of significant selective withdrawal , and
2. to determine the magnitude of the bias of the withdrawal flow for conditions other than those of complete selectivity.

The experimental design is shown in Figure 1.

Selective Withdrawal - General

Withdrawal of a fluid from a stratified flow field is of practical interest and has been seriously studied since 1949 (Craya). Selective withdrawal applications abound because many water properties in reservoirs and coastal waters vary significantly with depth. Selectivity refers to the ability of attracting a liquid of desired quality into an intake in preference to liquids from regions which are not of the desired quality.

The total volume of cooling water used for all industries in the United States is about 50% of all water use; all but 10% of which is accounted for by the power industry (11). Typically, the cooling water

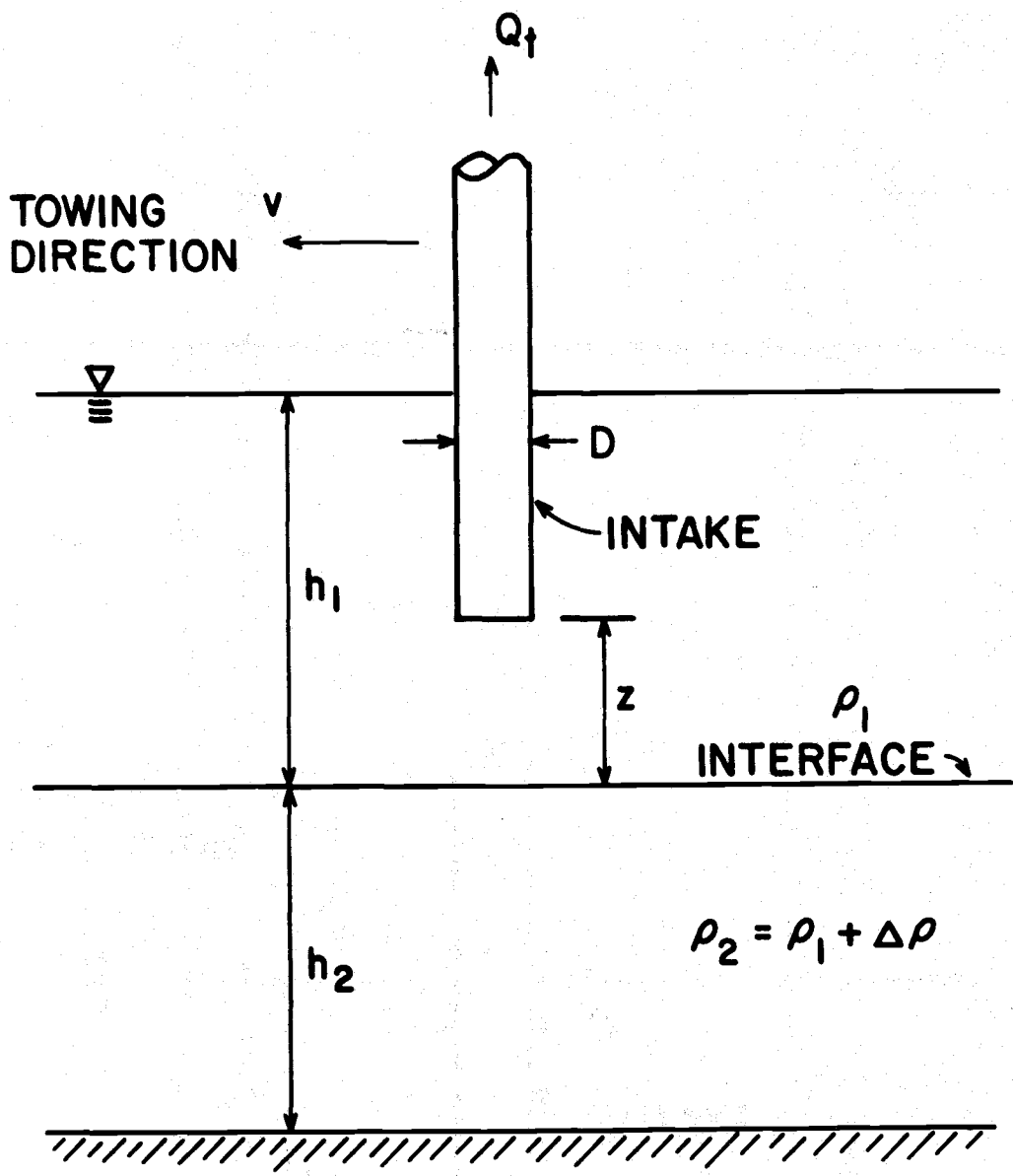


Figure 1. Experimental design

from these plants is discharged into the natural water bodies through which the waste heat reaches its ultimate sink, the atmosphere. Many theoretical and laboratory studies have suggested operating systems which could draw water from the cold lower region only, thus avoiding recirculation of heat energy. The published theoretical and laboratory studies of Craya (4); Gariel (6); Harleman, Morgan, and Purple (7); Yih (23); Debler (5); Huber (9); Kao (12); and Koh (15); are often cited as references for such design. However, these studies give consideration to only the fluid motion induced by the sink demand - an ambient current is not considered as a parameter. In marine environments and along the shores of streams and estuaries, an ambient current almost always exists; which might significantly influence the withdrawal phenomenon. Questions have been raised concerning the possibility of a significantly selective withdrawal flow in the presence of an ambient current.

Recirculation of heated water into the intake would significantly raise the temperature of cooling water of a thermal plant. Recirculation presents at least two detrimental effects: the efficiency of the plant is reduced and the temperature of the discharge water is even higher, increasing the potential harm to the environment. An increase in temperature would cause changes in the physical and chemical properties of water, such as: density differences would be produced which may cause stably stratified flows differing markedly from natural flow patterns; dissolved oxygen may be decreased; and biochemical reactions would be promoted by increases in water temperature. Increased surface temperatures may also have detrimental effects on higher level water species. Knowledge of occurrence of such consequences has promoted intake designs aimed

at reducing or completely avoiding the recirculation of heat energy associated with power plant installations.

In practice, the most common usage of selective withdrawal is for reservoir management. Intake structures are designed and placed near the level of the desired outflow so that the intake naturally draws fluid from that level. For example, an outlet located at the surface of a reservoir would be more likely to draw water of higher temperature and dissolved oxygen and lower turbidity, than would an outlet located near the bottom. The parameters most often controlled through selective withdrawal are temperature and dissolved oxygen. Many other physical and chemical properties are also considered; such as: turbidity, taste and odor caused by reservoir plant growth, salinity concentrations, fertilizer and pesticide residues.

#### Degree of Selectivity

A withdrawal flow is defined as selective if it shows a bias in favor of one layer or region over another. Further, the magnitude of the bias is defined as the degree of selectivity in reference to the layer or region of interest; and will be given the symbol  $S_i$ . The subscript signifies the region for which  $S$  is identified. The degree of selectivity,  $S_i$ , ranges from 0.0 to 1.0; a value of unity represents the special case of complete selectivity of withdrawal. For example, given  $S_i = X$  (dimensionless), 100X percent of the withdrawal flow is from the  $i^{\text{th}}$  layer while the remaining  $100(1-X)$  percent is from the other layer. The sum of the degrees of selectivity for all regions of the

flow field must have a value of unity:

$$S_1 + S_2 = 1.0 \quad . \quad (1)$$

The parameter used as a measure of the degree of selectivity must provide a reliable indicator of the relative magnitude of the flow from each layer within the withdrawal flow. A means of determining the magnitudes, when considering a two-layered flow field, is the tagging of each strata with a conservative tracer. Likely indicators are a tracer dye and the density of the strata itself. Simplicity in measurement and repeatable accuracy generally dictate the use of the density readings of each strata as the determinant for the bias.

Assuming that the strata's density may be considered a conservative property (that changes in temperature are negligible), the density of a sample of the withdrawal flow (assuming the components of the flow are sufficiently mixed) would then be related to the densities of both contributing flows.

Let  $Q_1$ ,  $Q_2$ , and  $Q_t$  represent the flows from the upper, and lower layers and the total discharge through the sink, respectively; and  $\rho_1$ ,  $\rho_2$ , and  $\rho_s$  represent the densities of the layers and that of the effluent sample. The following relation must hold from continuity principles:

$$Q_t \rho_s = Q_1 \rho_1 + Q_2 \rho_2 \quad (2)$$

If  $\Delta\rho = \rho_2 - \rho_1$ , the estimators are obtained as follows:

$$\begin{aligned} Q_t \rho_s &= Q_1 \rho_1 + Q_2 (\rho_1 + \Delta\rho) = (Q_1 + Q_2) \rho_1 + Q_2 \Delta\rho \\ &= Q_t \rho_1 + Q_2 \Delta\rho \end{aligned}$$

or

$$\rho_s = \rho_1 + \frac{Q_2}{Q_t} \Delta\rho = \rho_1 + \frac{Q_2}{Q_t} (\rho_2 - \rho_1)$$

and finally

$$S_2 = \frac{Q_2}{Q_t} = \frac{\rho_s - \rho_1}{\rho_2 - \rho_1}, \quad (3)$$

$$S_1 = \frac{Q_1}{Q_t} = \frac{\rho_2 - \rho_s}{\rho_2 - \rho_1}. \quad (4)$$

Thus, for a two-strata system, prior knowledge of the densities is sufficient for determination of the degree of selectivity; so long as the density of the respective fluids may be considered a conservative property.

#### Densimetric Froude Number

An oft used parameter which identifies the withdrawal flow is the internal or densimetric Froude number,

$$\frac{V}{(g \frac{\Delta\rho}{\rho} h)^{1/2}}$$

where

V - average velocity at the intake

g - gravitational acceleration

$\Delta\rho$  - change in density measured over some distance

$\rho$  - reference density of the fluid

h - reference length (such as the width or diameter of the



intake, or the distance from the intake to a reference depth or interface).

This parameter is a measure of the relative inertial to gravitational forces in the flow.

Generally, an increase in the intake Froude number will tend to decrease the selectivity of the flow. If the flow field has a linear density gradient it can be shown analytically that the width of the withdrawal layer increases with distance from the intake, when viscosity is considered (15). As the intake discharge is increased, the width of the withdrawal layer increases and the flow becomes less selective. An increase in the density gradient tends to decrease the width of the withdrawal zone.

Consider the two-layer system, as shown in Figure 1, having an intake located at some distance,  $z$ , above or below the interface. The densimetric Froude number provides a means of determining whether or not the interface is drawn to the intake (corresponding to whether or not a critical value of the intake Froude number has been reached). The value of the critical Froude number indicates the limiting conditions of fully-selective withdrawal. If the Froude number is below critical value, the flow is said to be fully-selective. If the Froude number is increased and both layers are homogeneous, the discharge from each layer becomes proportional to the respective depths of the layers. It should be noted that the conditions of fully-selective flow do not necessarily correspond with a value of unity of the degree of selectivity. If fluids are miscible and a horizontal velocity gradient is present in the region of the density-interface, vertical mass transport will occur and the

withdrawal flow will necessarily have a degree of selectivity less than unity.

### Literature Review - Selective Withdrawal

Since 1949 an increased number of studies were reported which were concerned with the withdrawal flow from a stable stratified fluid. The majority of these studies involved examining the fully-selective limits of withdrawal flows. Investigators sought to determine the critical conditions for complete selectivity of withdrawal into sinks of various types from flow fields having various stratification structures. The following literature review will be divided to consider first, the flow found in a two-layer system, and secondly, withdrawal from a flow field with a linear density gradient.

#### 1. Two-layer withdrawal flows

The first studies of withdrawal from a stratified flow field were those of Craya (4) and Gariel (6); which have been reviewed by Harleman (8) and Yih (24). Craya examined the critical conditions for fully-selective flow from a two-layer system into a horizontal intake located on a vertical boundary at an elevation greater than that of the stagnation interface. His studies included an orifice as well as a line sink. A solution for the analytic problem was obtained by a method using potential flow in contact with a stagnant fluid having a different density. A summary presented by Harleman (8) gave two expressions relating the critical withdrawal conditions, which are

$$\text{Orifice:} \quad \frac{V_c}{\left(g \frac{\Delta\rho}{\rho} D\right)^{1/2}} = 3.25 \left(\frac{z_0}{D}\right)^{5/2} \quad (5)$$

$$\text{Line Sink:} \quad \frac{V_c}{\left(g \frac{\Delta\rho}{\rho} D\right)^{1/2}} = 1.52 \left(\frac{z_0}{D}\right)^{3/2} \quad (6)$$

The parameter  $z_0$  indicates that this is the critical height for fully-selective withdrawal for the specified densimetric Froude number.

Gariel (6) experimentally substantiated these relationships for similar boundary conditions. The relationships are shown in Figure 2 in dimensionless form.

Davidian and Glover (as reported by Rouse (19)) examined the rate of flow necessary to initiate withdrawal from the lower region of a two-layer flow field with an intake located a distance above a density-interface. The situation was similar to that shown in Figure 1; with  $v = 0$  and  $h_1, h_2$ , large. At low discharges withdrawal occurred from the upper layer only. As the discharge increased, a critical value was reached at which flow from the lower layer started to enter the intake. By repeating the procedure for various heights above the interface, a relationship between the discharge and the critical intake-interface distance,  $z$ , for various density differences across the interface and various diameters of intake pipe was established. Both air-water and fresh water-salt water interface systems were examined. As indicated in Figure 2, the limiting condition for fully-selective withdrawal is:

$$\frac{V_c}{\left(g \frac{\Delta\rho}{\rho} D\right)^{1/2}} = 5.67 \left(\frac{z_0}{D}\right)^2 \quad (7)$$

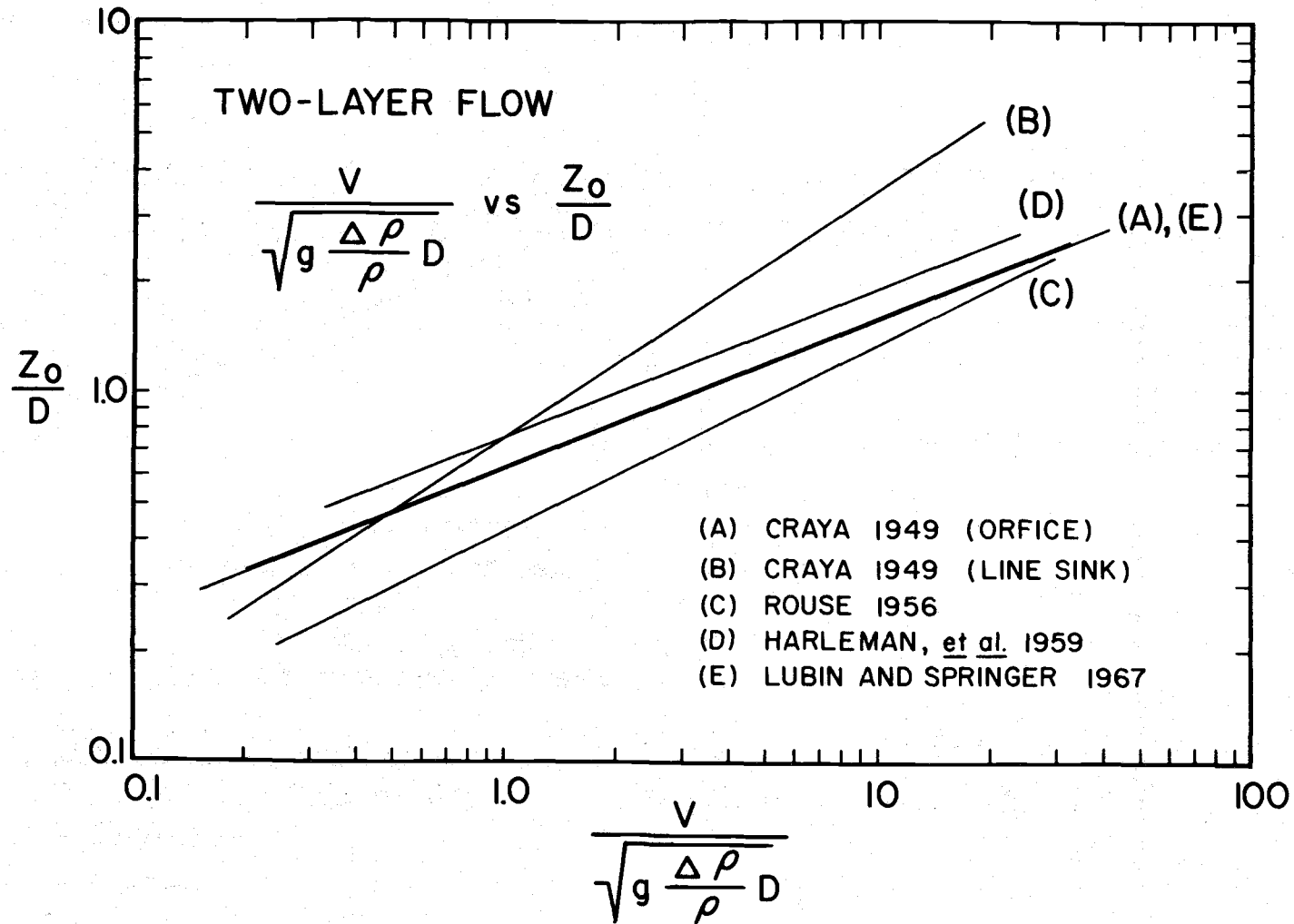


Figure 2. Critical fully-selective withdrawal conditions

Harleman, Morgan, and Purple (7) and Lubin and Springer (18) examined nearly identical flow conditions; Lubin and Springer included the effect of different immiscible fluids having various viscosities. Both studies investigated, analytically and experimentally, the efflux from a vertical circular intake in the bottom boundary to determine the magnitude of the critical discharge as a function of the fluid and geometric variables. For both studies the flow was assumed to be inviscid and incompressible; and discontinuities in density and velocity were allowed at the interface. The pressure across the interface was continuous and hydrostatic. Additionally, Lubin and Springer assumed the flow to be steady at the instant prior to the formation of the withdrawal cone.

Analytically, critical conditions for incipient drawdown were determined by Harleman, et al (7), by assuming a small change in the discharge would cause a large change in the intake-interface separation height measured immediately over the sink. The following expression was obtained for critical selective withdrawal:

$$\frac{V_c}{\left(g \frac{\Delta\rho}{\rho} D\right)^{1/2}} = 3.20 k \left(\frac{z_0}{D}\right)^{5/2} \quad (8)$$

where  $k$  is a proportionality constant signifying the amount the velocity at a point immediately over the intake on a hemispherical boundary must differ from the average velocity across the boundary. ( $k$  must be determined experimentally.)

Lubin and Springer (18) determined critical conditions for withdrawal from the lower layer only, by assuming the interface moves to the

intake instantaneously once critical conditions have been reached. (This assumption was justified observationally.) The following result for critical conditions was obtained:

$$\frac{V_c}{\left(g \frac{\Delta\rho}{\rho} D\right)^{1/2}} = 3.22 \left(\frac{z_0}{D}\right)^{5/2} . \quad (9)$$

The similarity of the relations obtained by Harleman, et al, (7) and Lubin and Springer (18) is not surprising because of the nearly identical withdrawal conditions examined. Corresponding plots of these relationships are shown in Figure 2, substantiated by closely fitting data ( $k=0.64$ ). The differences between the respective results may be attributed to the influence of viscosity and capillarity.

The theoretical and experimental work of Huber (9) and Huber and Reid (10) involving two-layer systems will next be discussed. They examined the withdrawal from a two-layer system through a line sink located in the bottom corner of a vertical boundary. The depths of the layers were equal (except in one case) while the densities were discontinuous. They assumed that the flows originated horizontally from a large reservoir; slip was allowed at the interface; and the pressure was continuous and equal across the interface. The method of solution for the analytic problem involved assuming the angle the interface makes with the horizontal at the intake, and subsequently determining the path of the interface from a relaxation solution with checks of the Bernoulli condition. The theoretical results were summarized in terms of the layer Froude numbers, where the reference lengths used were the respective depths of the two layers.

When flow into the intake was initiated, the bottom Froude number increased in value until the critical condition was reached. The critical value of the bottom Froude number,  $F_2$ , at which flow from the upper layer starts, is  $F_2 = 2.76$ . After this condition is reached, the Froude number of the upper layer increases while  $F_2$  decreases, reaching a low value of about 0.9. Further increases in the discharge causes increases in the Froude numbers of both layers, which remain equal for high values of discharge. Experimental results substantiated the latter prediction, but reveal a theoretical inadequacy at low rates of withdrawal. Reported test results show a flow from the upper region starting at a value of  $F_2 = 0.75$ , much lower than that predicted by the theory. An important conclusion of Huber and Reid's experiment was that the size of the sink was found to have little influence on the relationship of the Froude numbers. Yih (24) also acknowledged that the critical discharge is not sensitive to the size of the opening at the sink, so long as this opening does not become too large.

## 2. Linear density gradient

While the analysis of layered flow systems is applicable to some problems, the structure of many flow fields of interest may be approximated by a linear density gradient. This section reviews the work of Yih (23), Debler (5), Kao (12), Long (17), Koh (15) and Brooks and Koh (3). All have examined the withdrawal flow from a field characterized by a linear density gradient. Yih, Debler, and Kao have examined the phenomenon of two dimensional flow toward a line sink located at the bottom corner of a vertical boundary. This situation is similar to that used by Huber, discussed in the previous section. Debler (5) demonstrated experimentally

that when the densimetric Froude number of the flow is sufficiently low, the flow is characterized by the presence of a stagnant layer which is separated from the flow region by a line of velocity discontinuity. The critical value of the densimetric Froude number found by Debler is 0.28. Yih (23) has shown, through the use of potential flow theory, that for Froude numbers slightly greater than  $1/\pi$ , the separation of one part of the fluid from the rest is impossible. Yih's solution does not include a velocity discontinuity within the flow field, and for a Froude number slightly larger than  $1/\pi$ , the solution shows a large eddy which is nearly horizontal, resulting in a return flow far upstream. This solution is valid only for values of the densimetric Froude number (based on the total depth of flow) greater than  $1/\pi$  (0.318).

Debler's experimental results suggest that the proper solution for the flow with separation must incorporate a vortex sheet. This was lacking in Yih's analysis. Kao (12) examined the same situation and presented a free-streamline theory in which the fluid moving toward the sink is separated by a free-streamline from a completely stagnant region. In Kao's analysis the static upper layer is replaced by an equivalent moving layer flowing into a fictitious sink distribution. The required flow is that for which the pressure along the free-streamline is consistent with a static upper layer. Using this approach Kao was successful in examining the flow for Froude numbers less than  $1/\pi$ , the limit of Yih's solution. Kao found that all separated flows of the kind in question have a Froude number of 0.345 (based on the flowing depth of the layer); this is the case where selective withdrawal becomes possible. The difference in values of the Froude number for flow separation, found by Debler, Yih,



and Kao may be attributed to viscosity effects of the fluids.

Long (17) investigated the nature of the withdrawal flow toward a point sink located on a vertical boundary above the bottom in a linearly stratified flow field. He states "theoretical and experimental studies show that relatively fast motion will differ little from classical irrotational flows; as the motions become slower, velocity concentrations begin to appear. When speeds become very slow the fluid contains one or more jets which have the character of internal boundary layers. In these boundary layers the process of creation, advection and viscous diffusion of vorticity, strike a balance to permit the existence of the jets as a permanent feature of the motion." Experimental results reveal that the regions of velocity concentration adjust to such a width that the internal Froude number based on this width is of the order of unity. At lower values of the Froude number the intake draws more and more from its own level. The lowest value for which a solution exists, based on the channel depth, is  $1/(2\pi)$ . At this value a main jet forms in the middle of the channel and two counter-currents are found above and below. The ratio of the maximum velocity found in the main jet to that of the counter-currents is 3:1. At low levels of discharge the withdrawal is laminar; the jet is intense and the effects of friction and diffusion are deemed important. The behavior of vorticity is also interesting. The solution shows a generation of vorticity of two opposite signs carried into the jet from above and below. The result will be a build up of the observed shear, leading ultimately to an outward diffusion of vorticity sufficiently strong to just balance the influx.

The work of Koh (15) and that of Brooks and Koh (3) importantly

includes the influence of viscosity and diffusion on slow, steady withdrawal through a point or horizontal line sink located on a vertical boundary above the bottom. Koh's solution indicates the presence of a withdrawal layer symmetrically situated about a horizontal plane of the sink for both the two-dimensional and axisymmetric cases. The flow occurs from this layer, while outside it there is essentially no motion. The layer grows in thickness at a rate proportional with the 1/3 power of the distance from the sink. The velocity distributions are similar along the entire range of distance. Brooks and Koh (3) present an equation for a withdrawal thickness,  $\delta$ , under the stated conditions, as

$$\delta = 2.7 \left[ \frac{q}{(gE)^{1/2}} \right]^{1/2}$$

where  $q$  is the discharge per unit width,  $g$  is the gravitational constant, and  $E$  is the stability related to the density gradient. This formulation is perhaps the most widely employed description of the withdrawal phenomenon into a line sink.

#### Problem Formulation

Williams (22) states that within a marine environment "an ambient current almost always exists which would appear to prevent the possibility of significant selective flow." He relates that when the layers above and below the interface flow at velocities  $V_1$  and  $V_2$  respectively (see Figure 3), and

$$\frac{1}{2} (\rho + \Delta\rho) V_2^2 \approx \frac{1}{2} \rho V_1^2 \quad , \quad (10)$$

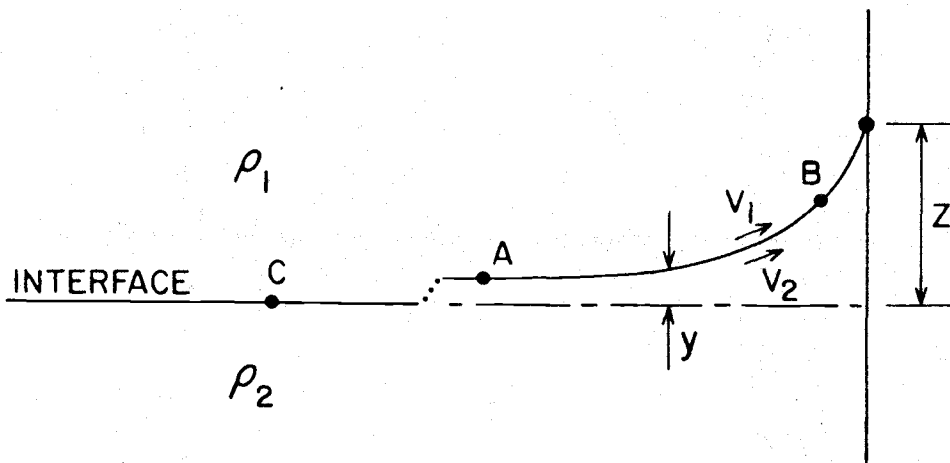


Figure 3. Configuration Discussed by Williams (22)

"there is no possibility of the intake drawing selectively and the proportion of each layer drawn in will correspond almost exactly with the proportion of their depths."

These above comments have provided the impetus and motivation for this study and it was decided worthwhile to explore this problem further. The following six assumptions are made in Williams (22) analysis:

- 1) the flow is inviscid
- 2) the flow is steady
- 3) the pressures across the interface are equal
- 4) both layers have roughly the same Bernoulli constant  
(they originated from the same quiescent source, such as a reservoir)
- 5) the datum for height measurements is the stagnation level of the interface;  $z = 0$  on the interface at point C

- 6) since the value of  $\Delta\rho$  is small,  $\frac{\Delta\rho}{\rho_1}$  is assumed equal to  $\frac{\Delta\rho}{\rho_2}$  without serious error.

With application of Bernoulli's equation along the interface, the velocities  $V_1$  and  $V_2$  are related by

$$\frac{1}{2} \rho_1 V_1^2 - \frac{1}{2} \rho_2 V_2^2 = g \Delta\rho z \quad . \quad (11)$$

Letting  $\rho = \frac{1}{2}(\rho_1 + \rho_2)$ , the following is obtained:

$$z = \frac{V_1^2 - V_2^2}{2 \frac{\Delta\rho}{\rho} g} \quad , \quad (12)$$

which relates that the difference in strata velocities is a measure of the distance the interface is from its stagnation level. At a point, such as A in Figure 3, this difference is a measure of the degree to which the flow is selective. Considering the conditions at point B, the velocities approach the high velocities required at the sink; the degree to which the flow is selective is determined by the angle at which the interface approaches the sink. Huber (9) examined the relation between this approach angle and the relative flow from each layer. Williams (22) relates that when an ambient current is present the stagnation level of the interface is not easily determined but is likely to correspond approximately with its actual flowing level, such that  $z \approx 0$  and selective flow is not possible.

In the process of obtaining equation (12) a number of questionable assumptions were made including: assumptions of equality of pressures across the interface and that of an invicid flow. Two streamlines have

equal pressures only if they are adjacent; which can occur in a viscous flow only if they are moving at about the same velocity. For two adjacent streamlines located above and below an interface with zero velocity in each strata, the pressures are continuous and equal on both sides of the interface because the streamlines are effectually at the same level. As long as this assumption is held for all conditions, these streamlines must remain adjacent with the interface located between. The change in velocity is then a measure of the change in interfacial height. The interface will usually reach the sink if there is a difference in velocities because the required velocities at the sink are very large and the change in interfacial height is a function of the square of these velocities. The assumption that the fluids are inviscid is questioned because viscosity is responsible for all motion in the lower strata when flow conditions correspond to those of complete selectivity. Viscosity allows shearing forces between vertically adjacent streamlines, which correspondingly serves as the mechanism for the diffusion of velocity through the layers and the creation of vorticity. The studies of Koh (15) and Long (17) concern such effects of viscosity.

This study examines the way in which the selectivity of withdrawal flow into a point sink suspended in the upper strata is affected by an ambient current in a two-layer system. The goals of this study are

1. to determine whether the presence of an ambient current does inhibit the possibility of significant selective withdrawal, and
2. to determine the magnitude of the bias of the withdrawal flow for other conditions than that of complete selectivity.

The problem may be formulated as one of determining the relationship

between the degree of selectivity and

1. the vertical distance separating the intake and the interface,  $z$ ,
2. the change in density across the interface,  $\Delta\rho$ ,
3. the discharge through the intake,  $Q$ ,
4. the diameter of the intake,  $D$ , and
5. the velocity of the intake relative to the undisturbed flow field,  $v$ .

The situation is that of Figure 1.

## II. EXPERIMENT

### Laboratory Equipment

The withdrawal flow from a two-layer system was examined. The laboratory configuration follows that shown in Figure 1. The study goals included determination of the influence of an ambient current on the selectivity of the withdrawal flow; as well as the dependence of the selectivity on the separation elevation of the density-interface and intake, and the change in density measured across the interfacial region. The experimental equipment consisted primarily of a cylindrical intake structure mounted on a towing bar located over the surface of an open tank. The intake hose connected with a pump and regulating valve, and finally to a drain (or second tank). The ambient current was simulated relatively by towing the intake structure over the surface of the water. In all cases, the upper fluid was tap water and the lower fluid consisted of a saline solution of various concentrations.

Two separate set-ups were used, the first of which was abandoned because of inadequacies in size. The tank dimensions in the first set-up were: 1.83 x 0.64 x 0.61 meters (72 x 25 x 24 inches). The discharges through the pumps and the dimensions of the intake diameters were: 12.7, 85.8, and 245 cubic centimeters per second and 0.38, 0.65, and 1.09 centimeters, respectively, for three groups of runs. During the last of these it was noticed that the readings of the intake-interface separation height,  $z$ , were not obtained accurately because the elevation of the density-interface changes substantially with each run. Also, motion in

the intake region was very slight and difficult for observation. The set-up was abandoned for one of a larger scale.

The second set-up included a flume having dimensions: 7.62 x 0.46 x 0.56 meters (25 feet x 18 inches x 22 inches). The pump used was capable of maintaining a steady discharge of 1300 cubic centimeters per second through an intake of diameter 3.175 centimeters (1.25 inches) and a discharge of 1220 cubic centimeters per second through an intake of diameter 2.54 centimeters (1 inch). The resulting flows were easily observable for measurement.

In the first set-up the motor responsible for towing the intake structure had a variable speed, and the intake was pulled at velocities of up to 5 centimeters per second. The motor was capable of reaching greater speeds but with the intake located so close to the density-interface, the interface was easily disturbed. In the second set-up the motor was geared at specific speeds. The speeds of towing varied from 0.80 centimeters per second to over 20 centimeters per second. The experimental set-up is diagrammed in Figure 4.

The process of obtaining a two-layer system with a distinct density-interface was the most critical aspect of the experiment. For miscible fluids there are two possible methods of creating a satisfactory interface. The first is to lay the fluid of lighter density on top of the heavier fluid, while the second is to introduce the heavier fluid beneath the one of less density. The latter method was chosen. The saline solution was mixed in a 1041 liter (275 gallon) cylindrical tank and introduced into the flume through two standpipes. Two plexiglass standpipes were designed as shown in Figure 5. The base was set on four 1.27 centimeter



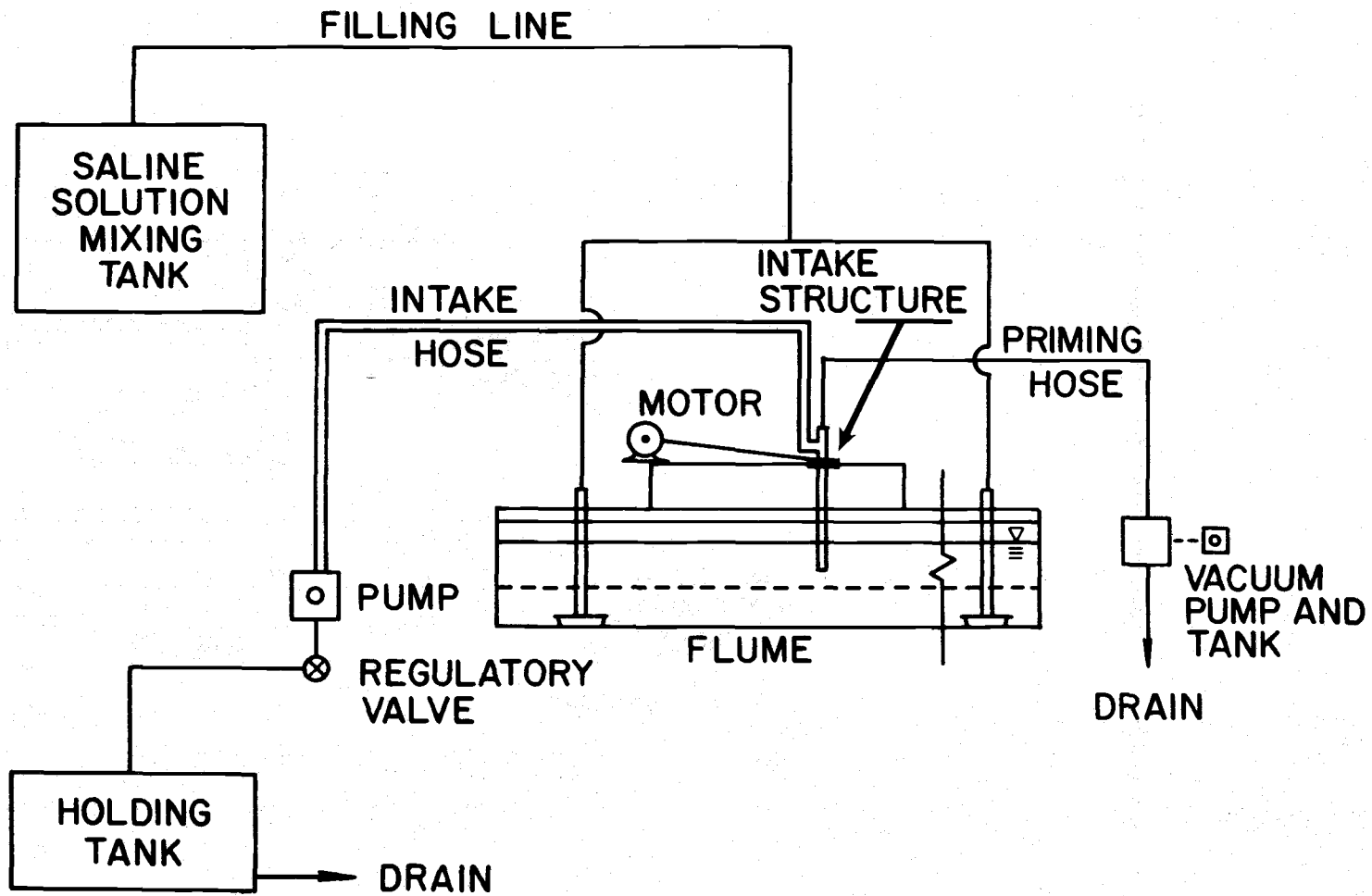


Figure 4. Experimental set-up

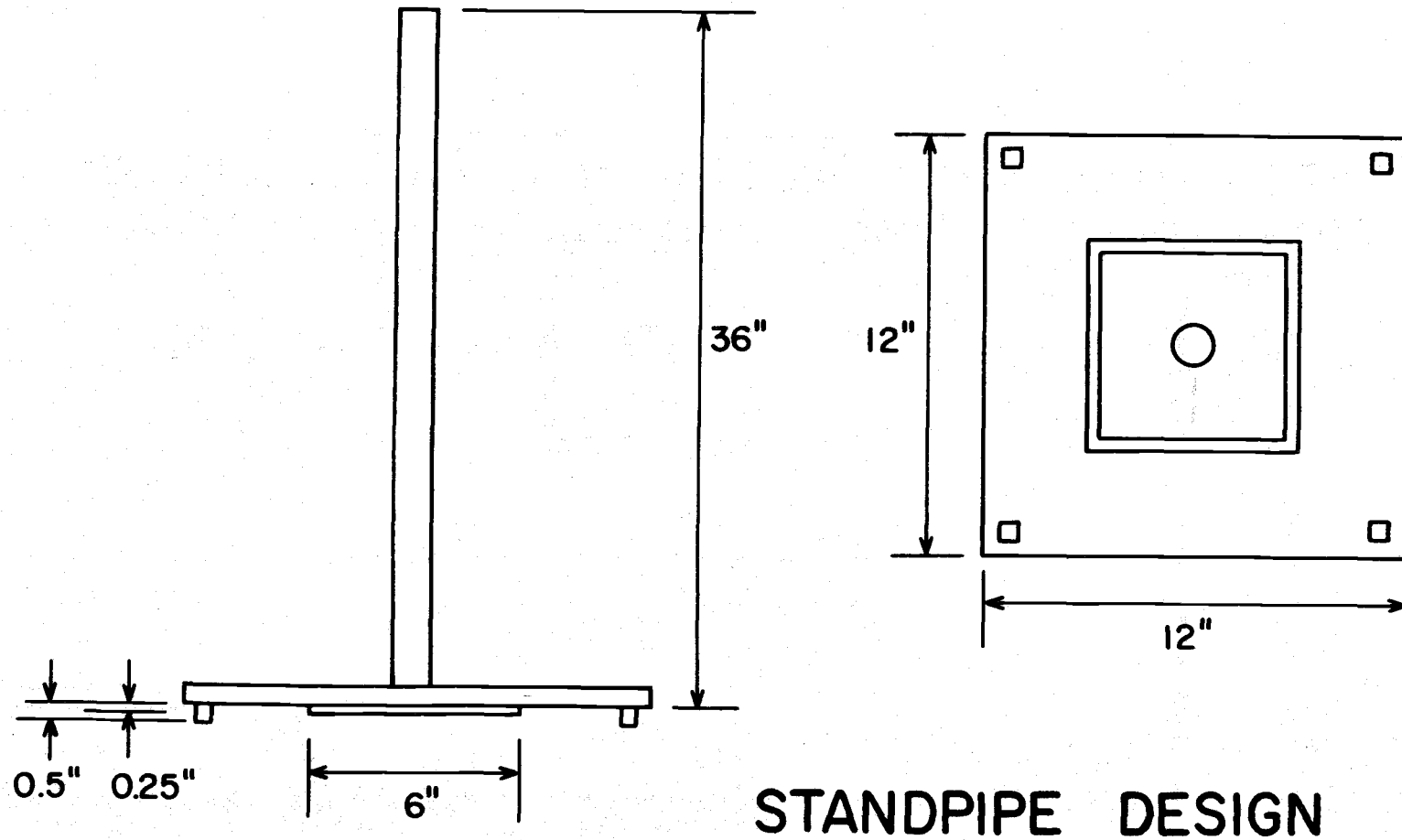


Figure 5. Plexiglass standpipe design

thick supports located in each corner. A 15 centimeter plexiglass square of 0.64 centimeter thickness surrounded the center hole. The purpose of the square was to catch and prevent air bubbles from flowing beneath the base of the standpipe and up through the density-interface. The original standpipes did not have this surrounding square and the air bubbles, in many cases, destroyed the density-interface before the run was started.

The saline solution, being of greater density, spreads slowly beneath the upper fluid when introduced through the standpipe. As long as the flow rate was maintained very low, little mixing of the interfacial region was experienced. In the experiment the flow rate was kept low until the depth of the lower layer exceeded that of the base of the standpipes. The flow rate was then increased. The upper strata was lifted by the incoming fluid until the desired depths were reached. Filling was terminated and the flume left for a period of time (usually about an hour) to allow internal currents to subside.

Before each test on the second set-up the intake hose and pump had to be primed. This was accomplished by attaching a second pumping system to the highest point of the intake structure. The second system consisted of a vacuum tank and an air pump with a connecting hose. The discharge through this system was very low.

### Procedure

The preparation for a run took a period of about six hours. The procedure was as follows:

1. The mixing tank was filled with tap water to a level of about 750 liters (200 gallons). The desired amount of salt (pellets for recharging water softeners) was added and mixed with a stirring motor until all the salt was in solution. If the salt solution was to be dyed, the dye was added at this time. For both set-ups, the dye used was Erioglaucine A Supra.
2. The flume was filled to a depth of about 30 centimeters with tap water and left to settle.
3. The filling line was assembled (made of garden hose with a dividing piece). Density samples from the flume and mixing tank were taken and recorded.
4. The mixing tank was located at a greater elevation than the flume so once the inflow to the flume was started in the filling line it continued under its own power. The flow was initiated through the filling line and divider and continued through each end piece into a drain. The flow was shut off in one piece of the line from the divider and this piece was placed in the top of the standpipe. The flow was restarted through this section at a very low rate. The same procedure was repeated for the other end of the filling line. The flow was left at a very low rate until the depth of the lower layer exceeded the elevation of the base of the standpipe. Once this point was passed the rate of inflow may be increased with no danger of mixing along the density-interface.
5. Once the desired depths were reached the inflow was terminated and the flume was left for a period of time. Following this static

period the run was started.

The run procedure took a period of about three hours. Tests were made in series of approximately equal height separations,  $z$ . The intake structure allowed adjustment of this height. With the height set, a test was performed with the intake held stationary. Tests were repeated at increasing speeds of the towing motor; so the simulated current appeared to increase. The height,  $z$ , was checked between each test and recorded. Adjustments were made when necessary. The procedure for an individual test was as follows:

1. The interfacial height was determined with a point-elevation caliper attached to the flume. The point was raised and lowered with a dial, the elevation being read directly. If neutrally buoyant spheres were used, they were placed on the interface and the point was aligned with them. If not, the point was aligned with the dye interface (which always remained distinct). The elevation was recorded. (The use of the spheres is explained in the next section.)
2. The surface elevation was read and recorded.
3. The vacuum tank was emptied.
4. The camera was adjusted and the lights adjusted and turned on.
5. The vacuum pump was started and the intake flow started at a very low rate.
6. Once the intake pump and hose were primed, the intake pump was started, the movie camera started, the motor pulling the intake structure started, and the vacuum pump turned off. The circuitry

was such that this could be controlled by one switch, simultaneously.

7. Once the desired motion appeared to be developed a density sample was taken from the end of the intake hose. Time was allowed for the desired withdrawal parcel to move through the entire intake hose system.

8. The motion of the towing carriage relative current was terminated and the flow through the intake hose reduced slowly through control of the regulatory valve. This could be accomplished so that disturbances of the interface due to the elimination of pressure concentrations were minimal.

9. A period of time was allowed for interfacial wave motion to subside. This was easily observable by watching the dye interface, or particularly by observing one of the neutrally buoyant spheres for a period of time.

10. The density of the sample was measured and the procedure repeated.

#### Methods of Observation - Analysis

Two types of observations were made on the tests of each run. The first of these involved sampling the withdrawal flow, which was taken for density determination. This provided a measure of the selectivity of the withdrawal flow. The second type of observation consisted of movies of the flow field in the vicinity of the intake. Various techniques of flow visualization were utilized. When dye had been added to the saline solution during mixing, the visual interface remained very distinct

throughout a run. Wave motion was easily observable, along with the motion associated with the intake cone.

On a number of tests a dyed immiscible solution of carbon tetrachloride and benzene was used. This immiscible solution was adjusted so that its density was between that of the upper and lower layers. If the solution was introduced through the upper surface with a syringe, spheres formed which fell to the level of the density discontinuity to remain on the level at which they were neutrally buoyant. The sphere size could be controlled to allow easy visualization. The movement of a sphere at any time would represent a streamline of the flow field. A stationary intake results in a steady flow field, while an ambient current changes the flow field to an unsteady one (unless the flow is considered from a coordinate system moving with the intake).

Introduction of spheres of slightly different densities allowed measurement of the thickness of the interfacial region. This technique also allowed for visual observation of interfacial shear. With the aid of the spheres, interfacial motion was easily recorded.

If potassium permanganate crystals were dropped through the layers, a dye streak remained which was used for velocity profile determination of the upper region.

The methods of analysis consisted primarily of determination of the sample density on a Christian Becker torsion balance capable of producing readings to the ten-thousandth of a gram per cubic centimeter; and observation of the movies. By plotting the observed movement at finite time intervals the velocity field could be determined under various conditions.

## III. FLOW PHENOMENA

Interfacial Shear and Associated Density Transport

The possibility of significant selective withdrawal from a two-layer flow system is dependent upon the strength of the withdrawal flow (sink demand) and its associated inertial forces, relative to the gravitational forces associated with the density-interface. Under conditions of fully-selective withdrawal the acting inertial forces along the density-interface are not of sufficient strength to overcome the gravitational forces, and the interface retains its approximate position in the flow field. The change in velocity from the flowing upper layer to the stationary lower layer is concentrated in the interfacial region. In the vicinity of the sink, the density-interface is exposed to an intense shear, while at a distance from the sink the shear may be negligible.

The presence of the region of shear implies that viscous forces are important in the interfacial region. Batchelor (2) relates two characteristics of viscous flows. The first states that "there is a gradual spreading or diffusion of velocity variations across streamlines, which comes about through the tangential force exerted across planes normal to the y-axis" (for assumed uni-directional flow in the x-axis direction). The rate of the diffusion of velocity decreases with time because the velocity gradient becomes progressively smaller. The second characteristic is that "the velocity distribution in the layer tends asymptotically to a similarity form depending  $\frac{y}{(\nu t)^{1/2}}$  alone, irrespective of the initial form of the transition." The variable  $\nu$  is the kinematic viscosity,



having units of length squared per time; and is a measure of the ability of molecular transport between adjacent fluid elements to eliminate a non-uniformity in the velocity field. The velocity profile resulting from the presence of a shear region is of a form similar to a centered error function.

Keulegan (14) discussed the shear region between two fluids of varying degrees of dissimilarity with the upper layer flowing over a stationary lower layer. The velocity distribution, thickness, and flows in the laminar boundary layers at the interface were determined, and three types of motion found. When the relative velocity between the layers was small, the interfacial surface was sharp and distinct. This indicates the densities are discontinuous and that the flow is laminar (though no restrictions were placed on the type of flow in the upper layer). As the relative velocity is increased a critical condition is reached at which the smoothness of the interface disappears and the interface becomes covered with waves travelling in the direction of the current with a velocity slightly less than that of the upper layer. When waves first appear, their crest lengths are longer than the distance between successive crests. At this stage, the waves are stable and travel with practically no deformation. If the relative velocity is increased, the crest lengths become shorter and the waves are sharp-crested. These waves are not stable and portions of the crests break, are thrown into the upper strata, and move forward and upward. As the relative velocity is increased, mixing of the lower layer into the upper layer occurs. At this stage, the wave length is no longer affected by changes of velocity.

A number of mechanisms of density transport are associated with the various conditions of shear. Keulegan (14) mentions the existence of a weak current in the lower layer flowing upward toward the interface. "In a sense, the boundary layer of the upper liquid acts as a pump, raising the small portions of the lower liquid to the level of the interface, then causing these portions to move horizontally." This current is associated with laminar flow, and as long as it is undisturbed, the steadiness of the boundary layer is assured. The vertical current is responsible for decreasing the selectivity of the withdrawal flow, in the present experiment, when conditions suggest that the withdrawal should be fully-selective.

### Interfacial Waves

Internal waves are important because of their influence on the withdrawal flow in the presence of an ambient current. Rumer (20) mentions that "the interfacial shear caused by the internal waves tends to increase vertical turbulent diffusion over that due just to diffusive mechanisms in the absence of internal waves." In a withdrawal flow this increase in vertical turbulent diffusion is expected to cause a decrease in the degree of selectivity, over that found in the absence of the waves.

When considering interfacial waves in a two-layer system the effect of the upper strata is to diminish the celerity of interfacial waves of any length according to the ratio

$$\left[ \frac{\rho_2 - \rho_1}{\rho_2 + \rho_1} \right]^{1/2}$$

This is because of a decrease in the potential energy of a given deformation on the interface according to the ratio  $(\rho_2 - \rho_1) : 1$ , coupled with an increase in kinetic energy in the ratio  $(\rho_2 + \rho_1) : 1$ . An interfacial disturbance, as compared to a disturbance on the free surface, would cause a large amplitude deformation on the interface which would be expected to move at a slow velocity.

#### Creation of Waves by a Moving Disturbance

The creation of waves by a point disturbance of a free surface has been discussed by Lamb (16). The generated waves increase in length as they leave their source area (and thus the waves accelerate as they move, due to the dependency of the celerity on wave length). At any location away from the source the wave period decreases with time while the wave amplitude increases. When the initial disturbance is spread over a finite area, the wave length at the source decreases with time and eventually reaches a size where its dimensions are comparable to those of the disturbance. At this time, different parts of the disturbance are no longer in phase and the waves interfere with each other. The increase in amplitude is arrested and the disturbance dies out.

Considering an arbitrary distribution of pressure located over a stream which is moving with velocity,  $c$ , the resulting motion may be understood in terms of a disturbance acting as a number of infinitesimal disturbances applied equidistantly at infinitesimally close locations and intervals. Each disturbance will produce a system of waves, the resultant of which is the superposition of all the so produced systems. The con-

sequence of this is that the wave which is created is due only to those portions which reinforce one another. These are the portions which have a wave celerity equal to the velocity of the stream. This result is important for whenever the disturbance moves with a velocity relative to the undisturbed flow, the waves which are created have celerity equal to the relative velocity of the disturbance.

If the influence of depth is incorporated, the problem is one of whether the stream velocity,  $c$ , is greater or less than the maximum wave velocity for the given depth,  $(g h)^{1/2}$ , where  $h$  is the depth. For the case in which  $c^2$  is greater than  $(g h)$  the roots of the equation are imaginaries, and it appears that the surface elevation (which is symmetrical with respect to the origin) is insensible beyond a certain distance from the disturbance. For that case for which  $c^2$  is less than  $(g h)$ , the problem is indeterminate, though the principal value for the state of steady motion may be found. At a distance following the disturbance the deformation of the surface consists of a simple-harmonic train of waves; the length of the individual waves corresponds to a celerity of propagation,  $c$ , relative to the still water.

If a low-pressure disturbance moves over an otherwise still surface at a velocity,  $c$ , the individual waves which are created have a velocity equal to that of the disturbance. Groups of waves are left behind the disturbance because the group velocity is less than the velocity of the individual waves (Lamb (16) Art. 236).

For all cases examined, if the velocity of the pressure disturbance is less than that of the minimum wave velocity, given by Lamb (16) in equation 5, article 267, no waves will be generated on the surface.

Wiegel, Snyder, and Williams (21) examined the generation of gravity waves on a free surface by a moving low-pressure area in a towing tank. They noted that "waves generated in this manner had a phase velocity identical to the velocity of the moving low-pressure area." Theory (based on linear wave concepts) predicts the amplitude of the generated wave will increase from zero as the velocity of the moving low-pressure area,  $v$ , increases from zero to the shallow-water wave celerity,  $(g h)^{1/2}$ . When  $v$  is equal to  $(g h)^{1/2}$  the theory predicts an infinite wave amplitude. Their experimental results indicate that the generated wave amplitude increases with the value of the ratio

$$\frac{v}{(g h)^{1/2}}$$

until a value less than unity is reached; at which point the amplitude decreases with further increases in the value of the ratio. The results for the case of a low-pressure area length of two feet and a 1.06 foot water depth indicate the wave amplitude increases until the value of the above ratio reaches 0.86. Further increases in  $v$  show a decreasing wave amplitude. The discrepancy between the theory and experiment may be explained by noting that at large wave amplitudes linear wave theory becomes invalid.

For values of  $v$  less than  $(g h)^{1/2}$  Wiegel, et al. found that the generated waves have nearly a constant period, and a wave group is found behind the source. As the value of  $v$  approaches  $(g h)^{1/2}$ , the first observable wave appears to be solitary or cnoidal. This initial wave is followed by a group of smaller dispersive waves. Wiegel, et al.

performed tests with three lengths of the pressure area: 2, 4, and 6 feet. There was no apparent effect of the length of the low-pressure area on the wave velocity.

Figure 6 from Wiegel, et al. (21) shows the position of the generated wave relative to the centerline of the low-pressure area for various velocities of the moving low-pressure area. As the velocity of the low-pressure area increases, the crest of the generated wave is located further behind the centerline. This is important for the present study because the location of the interfacial wave crest appears to influence the degree of selectivity of the withdrawal flow.

For a stationary low-pressure area the laboratory results of Wiegel, et al, show that no waves are formed on the surface, which indicates that the generation of gravity waves is a function of the relative velocity of the pressure area and free surface.

### Capillarity

The effects for which the term capillarity is used are those due to molecular attraction at a fluid-fluid interface. There is a tendency for the fluid-fluid system to reach a state of minimum internal energy which requires that the surface area of the interface be a minimum. Any increase in surface area due to curvature causes a tangential stress which acts to eliminate the curvature. The magnitude of the stress between two adjacent portions of the surface, due to this molecular attraction or 'surface tension', depends only on the nature of the two fluids and on the temperature.

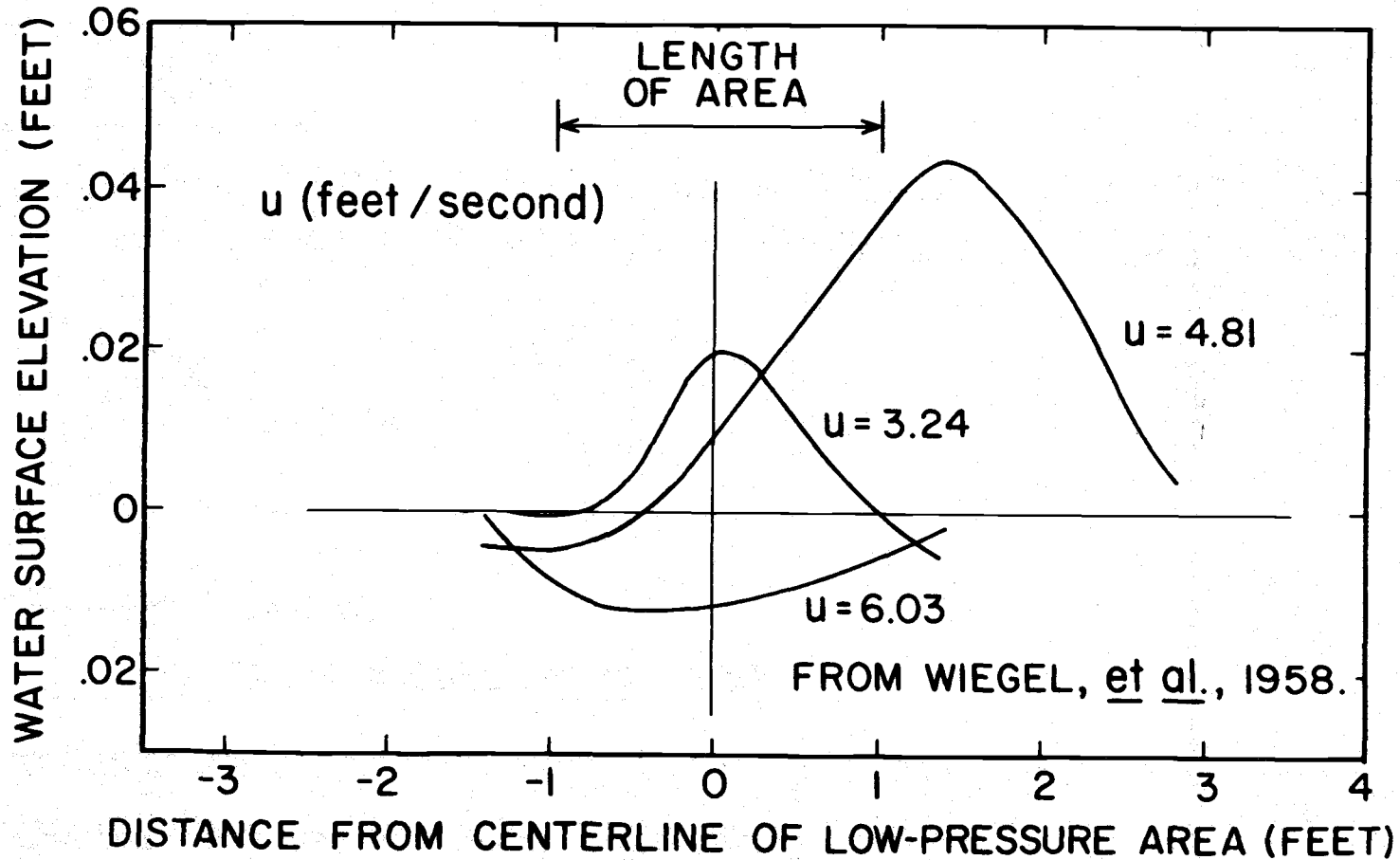


Figure 6. Position of generated wave

Abraham (1) examined the scale effects due to surface tension for model studies of gravity waves generated by a moving pressure distribution, and included a discussion of the wave pattern generated by a moving circular low-pressure area (also discussed by Lamb (16) Art. 256 and 272). Abraham noted that the waves, which are generated by the moving pressure distribution, travel with the same velocity as the pressure source, and in the same direction. The influence of surface tension depends on the ratio of the disturbance velocity to the minimum celerity of the waves. When  $v$ , the pressure velocity, is not much larger than the minimum celerity of the waves,  $c_{\min}$ , the gravity and capillary waves which are generated are of the same order of magnitude and the resulting pattern is influenced by surface tension. The region within the asymptotes of the wave pattern is always influenced by surface tension while that outside the asymptotes is influenced only if the disturbance velocity  $v$  is less than  $3.2 c_{\min}$ . The relation for the asymptotes of the wave pattern, given in terms of the angle,  $\phi$ , which is made with the axis of movement is

$$\sin \phi = \frac{c_{\min}}{v}$$



#### IV. EXPERIMENTAL RESULTS AND DISCUSSION

This study examined the way in which the selectivity of flow withdrawal into a vertically suspended, upper strata point sink is affected by an ambient current in a two-layer system. The goals were

1. to determine whether the presence of an ambient current inhibits the possibility of significant selective withdrawal;
2. to determine the magnitude of the bias of the withdrawal flow for conditions other than those of complete selectivity.

The experimental design and relevant parameters are shown in Figure 1.

In this section experimental results of the study are presented. The discussion primarily concerns the withdrawal degree of selectivity and how it is affected by the density difference of the interfacial region, the proximity of the intake to the density-interface, and the relative velocity of the simulated current. A number of experimental observations are also mentioned and discussed. The study examined a wide range of conditions in which the density across the interfacial region was varied from 0.016 to 0.082 grams per cubic centimeter; the range of the separating height,  $z$ , varied from 1 to 9 centimeters; and the towing speed of the inlet tube varied from zero to 21.5 centimeters per second.

Linear Regression results are summarized in Table 1.

##### Influence of the Proximity and Density Differential Parameters

As expected, the degree of selectivity was found to be greatly dependent on the proximity of the intake to the density-interface;

TABLE I

DEPENDENT VARIABLE	INDEPENDENT VARIABLE(S)	DATA RANGE	REGRESSION EQUATION	R <sup>2</sup>
1. $Q_1/Q_t$	$Z/Z_c$	$0 \leq \frac{Z}{Z_c} \leq 1.0$	$Q_1/Q_t = .496 + .468 (Z/Z_c)$	0.920
2. $Q_1/Q_t$	$Z/Z_c, \Delta\rho/\rho_1$	$0 \leq \frac{Z}{Z_c} \leq 1.0$	$Q_1/Q_t = .468 + .472 Z/Z_c + .605 \Delta\rho/\rho_1$	0.932
3. $Q_1/Q_t$	$Z$	$0 \leq \frac{Z}{Z_c} \leq 1.0$	$Q_1/Q_t = .549 + .0720 Z$	0.742
4. $Q_1/Q_t$	$Z/Z_c, \Delta\rho/\rho_1$	$0 \leq \frac{Z}{Z_c} \leq 1.0$	$Q_1/Q_t = .415 + .0840 Z + 2.204 \Delta\rho/\rho_1$	0.875
5. $Q_1/Q_t$	$Z/Z_c$	$0 \leq \frac{Z}{Z_c} \leq 1.0$	$Q_1/Q_t = 0.41 + .723 \tanh(Z/Z_c)$	0.945
6. $Q_1/Q_t$	$Z/Z_c, \Delta\rho/\rho_1$	$0 \leq \frac{Z}{Z_c} \leq 1.0$	$Q_1/Q_t = .352 + .729 \tanh(Z/Z_c) + .265 (\Delta\rho/\rho_1)^{1/2}$	0.956
7. $Q_1/Q_t$	$Z/Z_c$	$0 \leq \frac{Z}{Z_c} \leq 1.7$	$Q_1/Q_t = 0.639 \text{EXP} [1.93 \tanh(Z/Z_c) - 1.07 (Z/Z_c)^{1/2}]$	0.941
8. $Q_1/Q_t$	$Z/Z_c$	$1.0 \leq \frac{Z}{Z_c} \leq 1.7$	$Q_1/Q_t = 0.916 + 0.038 Z/Z_c$	0.252
9. $Q_1/Q_t$	$\Delta\rho/\rho_1$	$1.0 \leq \frac{Z}{Z_c} \leq 1.7$	$Q_1/Q_t = 0.934 + .781 \Delta\rho/\rho_1$	0.377
10. $Q_1/Q_t$	$Z/Z_c, \Delta\rho/\rho_1$	$1.0 \leq \frac{Z}{Z_c} \leq 1.7$	$Q_1/Q_t = 0.882 + .818 \Delta\rho/\rho_1 + .040 Z/Z_c$	0.664
11. $\Delta\rho/\rho_1$	$Q_1/Q_t, \Delta\rho/\rho_1$	$0 \leq \frac{Z}{Z_c} \leq 1.1$	$\Delta\rho/\rho_1 = -0.089 + .335 Q_1/Q_t - .253 \tanh Z/Z_c$	0.205

measured by the variable nozzle interface separation height,  $z$ , (see Figure 1). The experimental results under the condition of zero ambient current are shown in Figure 7. Each point is labeled with the density difference of the test from which it is taken multiplied by 1000, ie.  $(\Delta\rho = \rho_2 - \rho_1) \times 1000$ . It is seen that points on the upper, left boundary of Figure 7 have a greater density than those data points on the lower right boundary. This suggests that if flow conditions are set, resistance to motion would be greater for a flow field having a greater density differential across the interfacial region. Subjected to equal pressure fields, a fluid with less density shows a greater acceleration. To obtain another relation similar to that found in Figure 7 the variable  $z$  may be divided by the critical proximity for complete selectivity of withdrawal,  $z_c$ , as reported by Rouse (19).

$$\frac{V_c}{\left(g \frac{\Delta\rho}{\rho} D\right)^{1/2}} = 5.67 \left(\frac{z_c}{D}\right)^2 \quad (13)$$

The above relation gives the minimum discharge (in terms of the velocity at the intake) at which the lower fluid as well as the upper fluid is carried into the intake; and was developed for either a liquid-liquid interface or an air-liquid interface. This expression may be transformed to yield

$$z_c = 0.474 \left[ \frac{Q}{\left(g \frac{\Delta\rho}{\rho_1} D\right)^{1/2}} \right]^{1/2} \quad (14)$$

where  $z_c$  is the critical height for fully-selective withdrawal given a discharge  $Q$  through the intake of diameter  $D$  with a difference in density

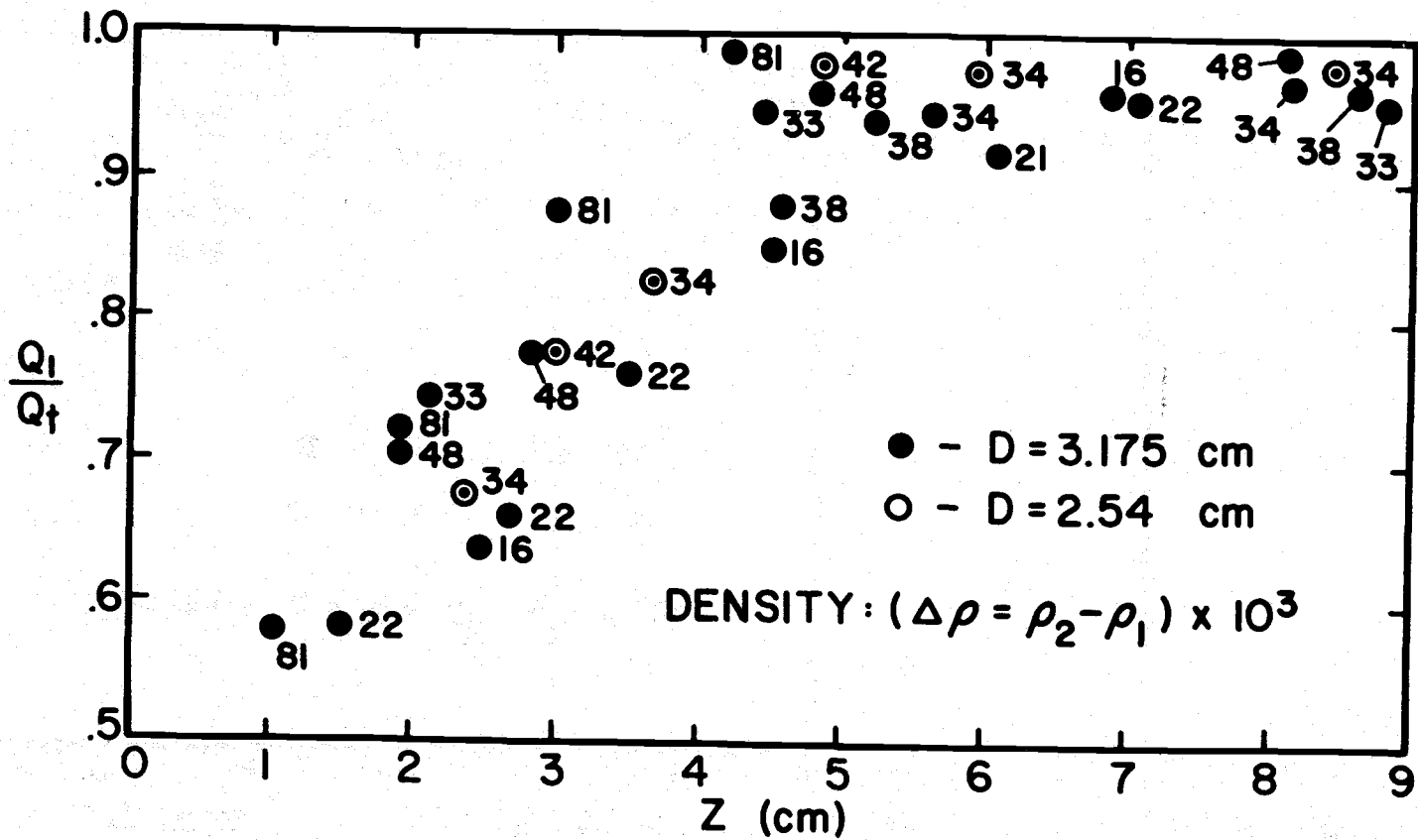


Figure 7. Relation of the degree of selectivity to the separating height

between the upper and lower layers of  $\Delta\rho$ .  $\rho_1$  is the density of the upper layer. Figure 8 shows the relation between the degree of selectivity and the dimensionless proximity parameter,  $z/z_c$ . It is apparent that values of  $z/z_c$  less than unity imply that the density-interface is drawn to the intake; while values greater than unity suggest that the interface does not reach the intake. Thus, different mechanisms are expected to be at work in the flow field, depending on the value of  $z/z_c$ .

When the data points for  $z/z_c$  less than unity are examined using linear regression techniques, it was found:

$$S_1 = \frac{Q_1}{Q_t} = 0.0496 + 0.468 \left(\frac{z}{z_c}\right), \quad (15)$$

labeled as curve A in Figure 8. The value of  $R^2$ , the coefficient of correlation which measures the proportion of the variation in the dependent variable which is accounted for by the fitted equation, obtained with this equation is 0.920. This means that 92% of the variability in  $S_1$  is explained by the given equation so long as  $z/z_c$  is less than unity. Curve B of this same figure is the resulting regression equation when all data points are considered. This equation is

$$S_1 = 0.639 \text{ EXP}[1.93 \tanh\left(\frac{z}{z_c}\right) - 1.07\left(\frac{z}{z_c}\right)^{1/2}] \quad (16)$$

The corresponding value of  $R^2$  is 0.941.

It is of interest to examine the cases of  $z/z_c$  greater than unity and  $z/z_c$  less than unity separately. Figure 9 shows the data for the latter case, where again the ambient current is zero. In this figure

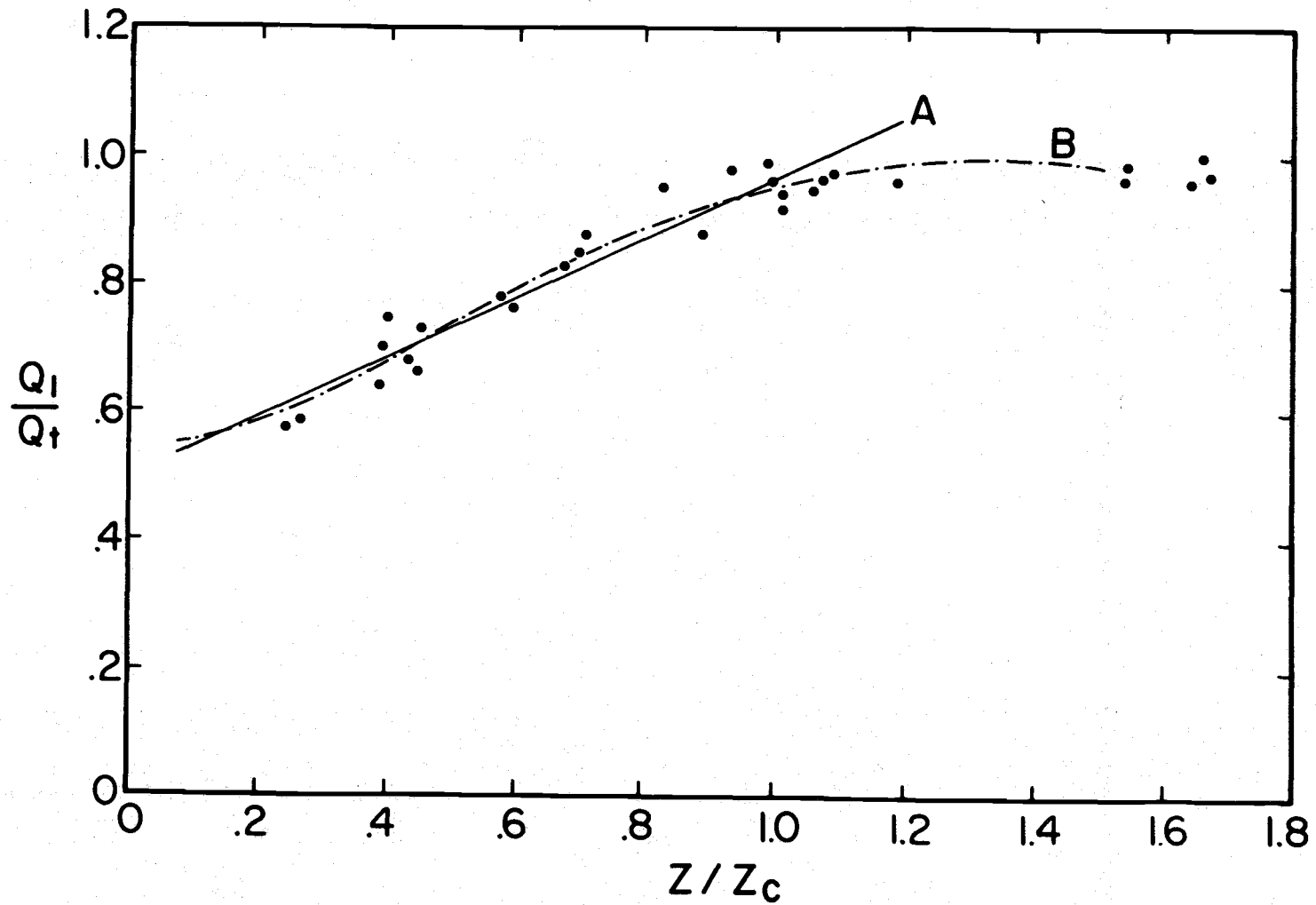


Figure 8. Relation of the degree of selectivity to the proximity parameter

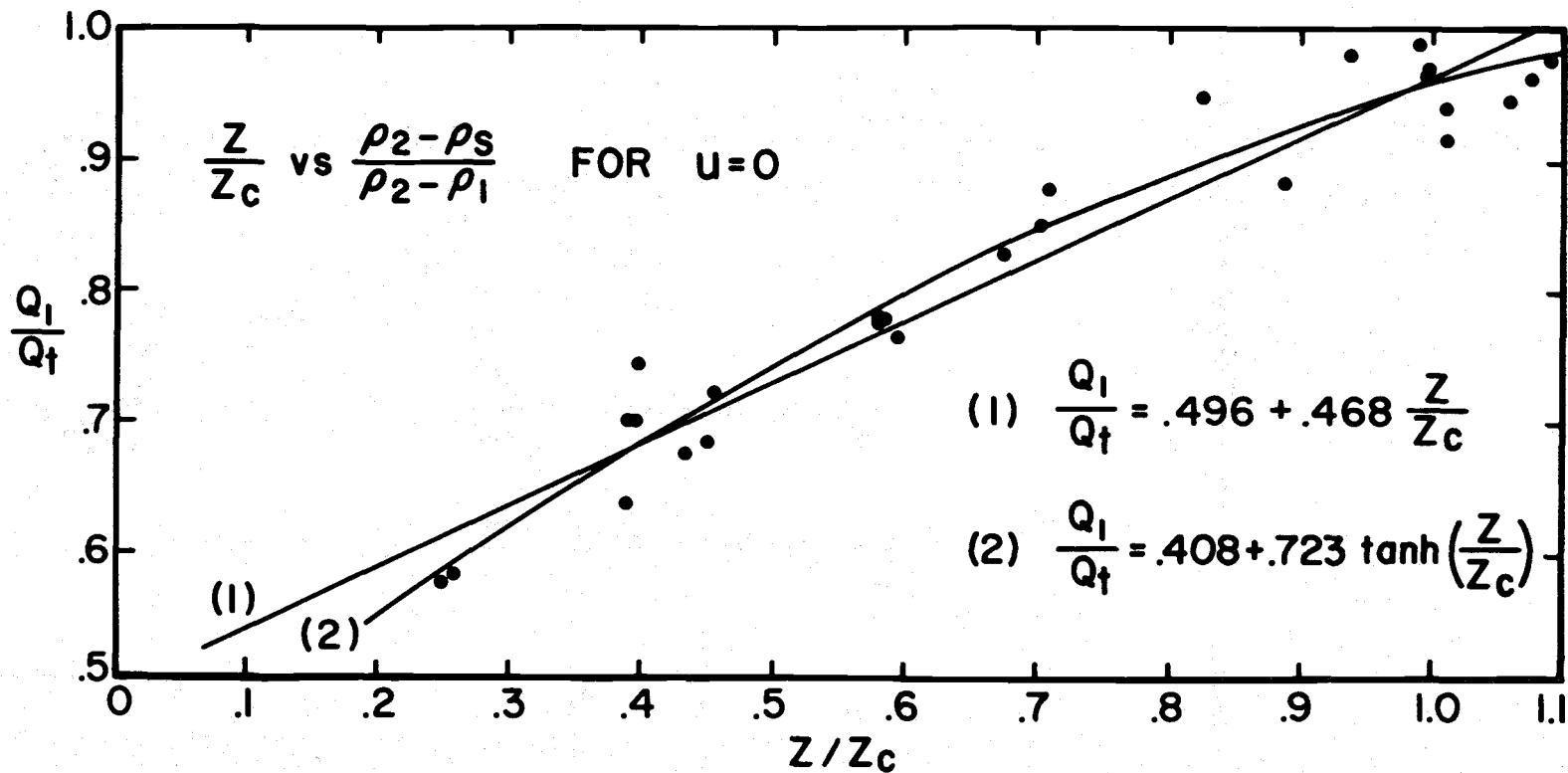


Figure 9. Relation of the degree of selectivity to the proximity parameter having range less than unity

a regression equation using a hyperbolic tangent is compared with the linear relation of equation (15). The expression using a hyperbolic tangent is

$$S_1 = 0.408 + 0.723 \tanh\left(\frac{z}{z_c}\right) \quad (17)$$

for which an  $R^2$  value of 0.945 is obtained, not much higher than that of equation (15).

Linear regression techniques were applied to data points for  $z/z_c$  less than unity to determine the influence of the density difference across the interface. The following was obtained;

$$S_1 = 0.352 + 0.729 \tanh\left(\frac{z}{z_c}\right) + 0.265 \left(\frac{\Delta\rho}{\rho_1}\right)^{1/2} \quad (18)$$

for which the value of  $R^2$  is 0.956. When compared to equation (17) it is apparent that the slope due to the proximity parameter,  $z/z_c$ , remains roughly the same (0.729 vs. 0.723). An increase in the density serves to increase the selectivity of the withdrawal flow for any given  $z/z_c$ . Figure 10 shows two curves with values of  $\frac{\Delta\rho}{\rho_1}$  of 0.02 and 0.06. A number of data points are also included for reference.

Within this range ( $0.0 < z/z_c < 1.0$ ) the product-moment correlation coefficients for  $S_1 : z/z_c$  and  $S_1 : z$  are 0.959 and 0.944, respectively. These high values of the correlation coefficients were obtained from data with values of the density differential parameter,  $\frac{\Delta\rho}{\rho_1}$ , ranging from 0.0160 to 0.0811. It is apparent that within this range of the proximity parameter the magnitude of the difference in densities between the layers is not important.

The mechanism of withdrawal from the lower layer when the proximity



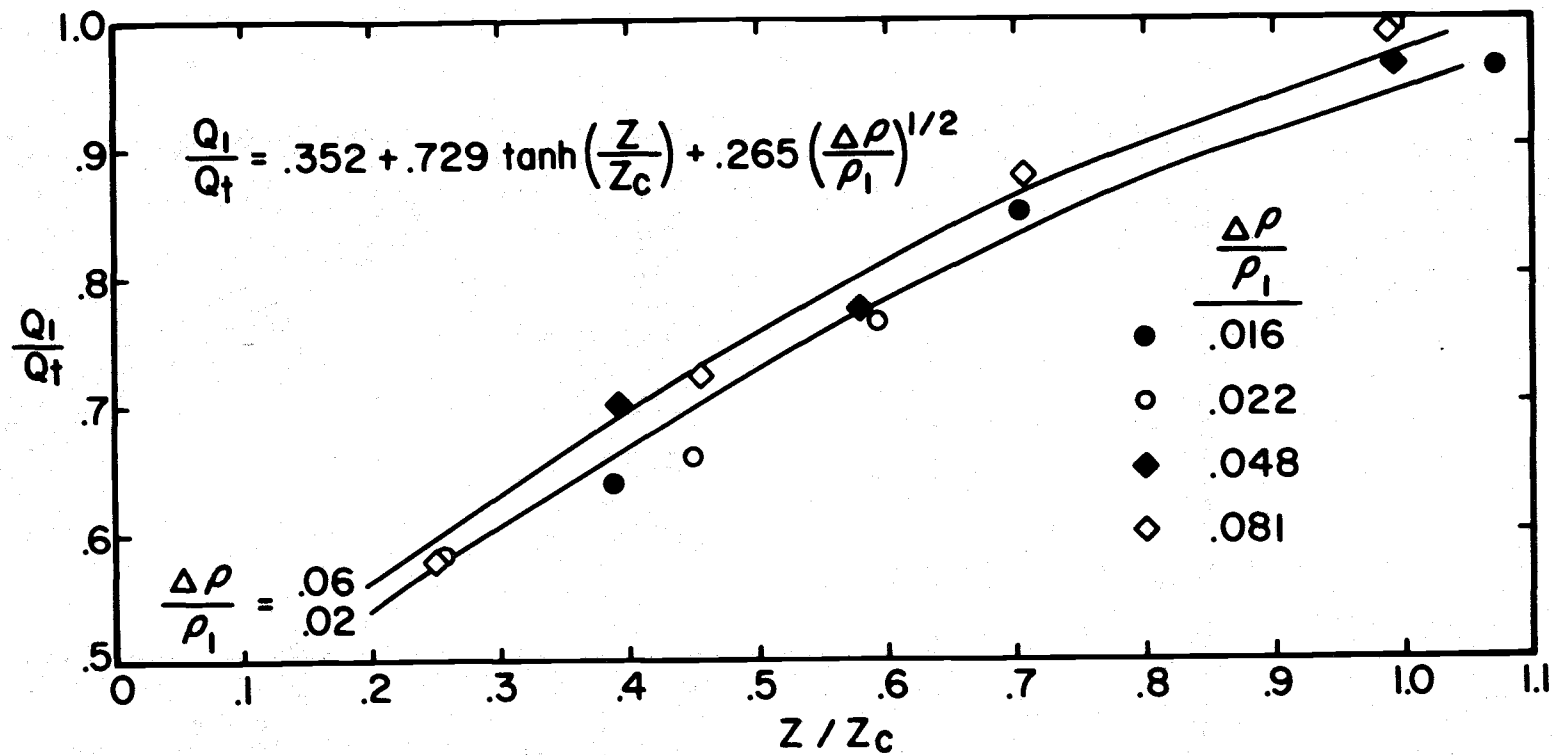


Figure 10. Influence of the density differential on the degree of selectivity; proximity parameter less than unity

of the intake to the interface is less than the critical value resembles potential flow into the intake. There was no observable circulation associated with this withdrawal flow. Figure 11 shows typical withdrawal cones for  $z/z_c$  values of 0.25, 0.46, 0.71, and 0.99. Picture 1 shows the cone having  $z/z_c$  value of 0.71. The shape of the withdrawal cone is seen to be a function of the dimensionless proximity parameter. Under these conditions the size of the withdrawal cone is determined primarily by the value of  $z/z_c$ . Figure 12 shows the relation between the proximity parameter and the diameter of the withdrawal cone (jet) measured at the mouth of the intake structure,  $D_c$ ; the latter of which has been made dimensionless by dividing by the intake diameter,  $D$ . This relationship appears to be linear. Also shown in Figure 12 is the relation between the proximity parameter and the minimum diameter of the withdrawal jet from the lower layer,  $D_c^*$  (similar to the vena contracta of flow through an orifice). The minimum diameter is located about one centimeter in from the mouth of the intake structure, which in this case is 3.175 centimeters in diameter. Figure 13 shows the relation between the degree of selectivity of the withdrawal flow and the ratio of the cross-sectional area at the vena contracta,  $A_c^*$  (the cross section where the contraction of the jet is the greatest) of the withdrawal jet to the cross-sectional area of the intake,  $A_1$ . As expected, this relationship is linear and the mentioned ratio could have been used as an estimator of the selectivity of the withdrawal flow in place of the defined degree of selectivity; so long as the proximity parameter is less than critical.

When the separating distance of the intake and density-interface is greater than the critical value at which the interface is drawn to the

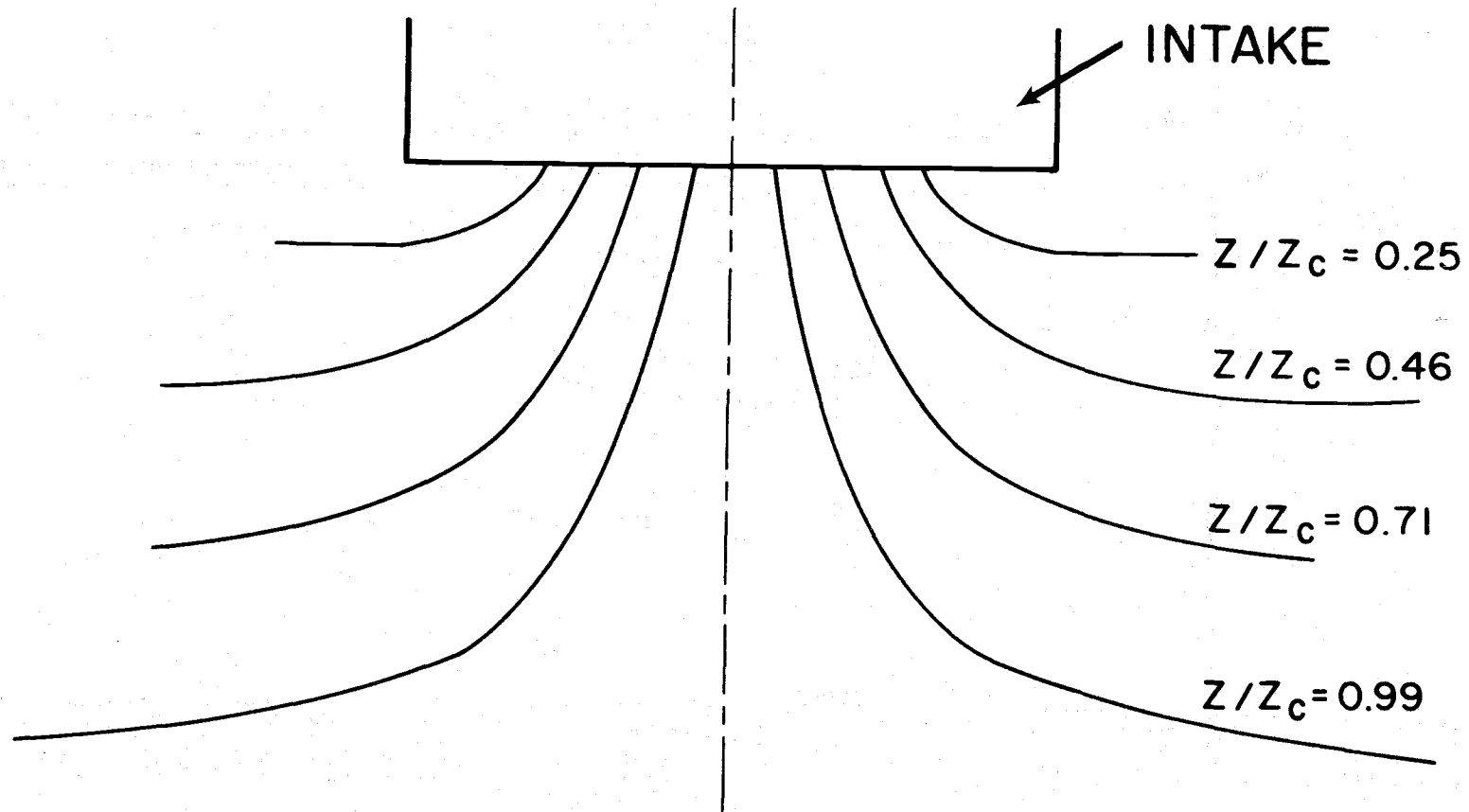
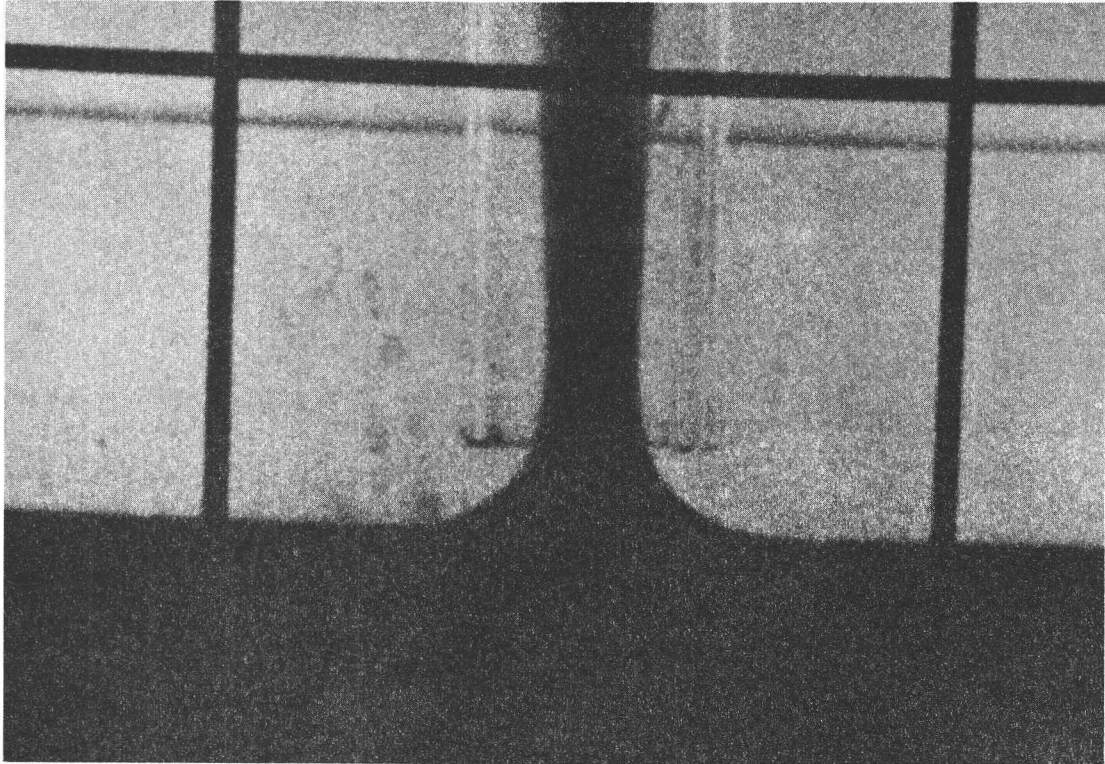


Figure 11. Typical withdrawal cones:  $\frac{\Delta\rho}{\rho_1} = 0.081, u=0$



Picture 1. Typical withdrawal cone:  $\frac{z}{z_c} = 0.71$  ,  $\frac{\Delta\rho}{\rho_1} = 0.081$  ,  $u = 0$

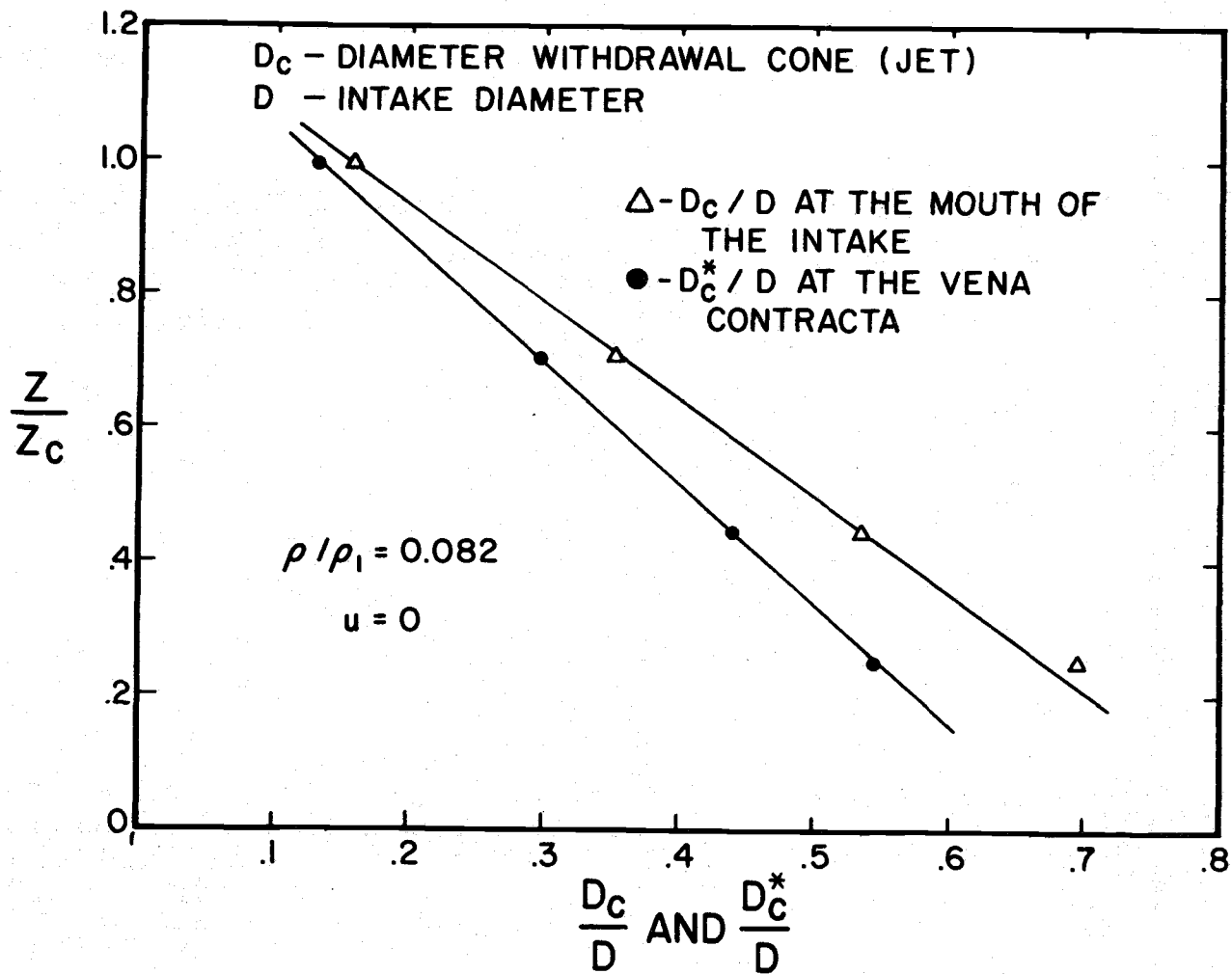


Figure 12. Relation of the proximity parameter to the intake diameter parameter

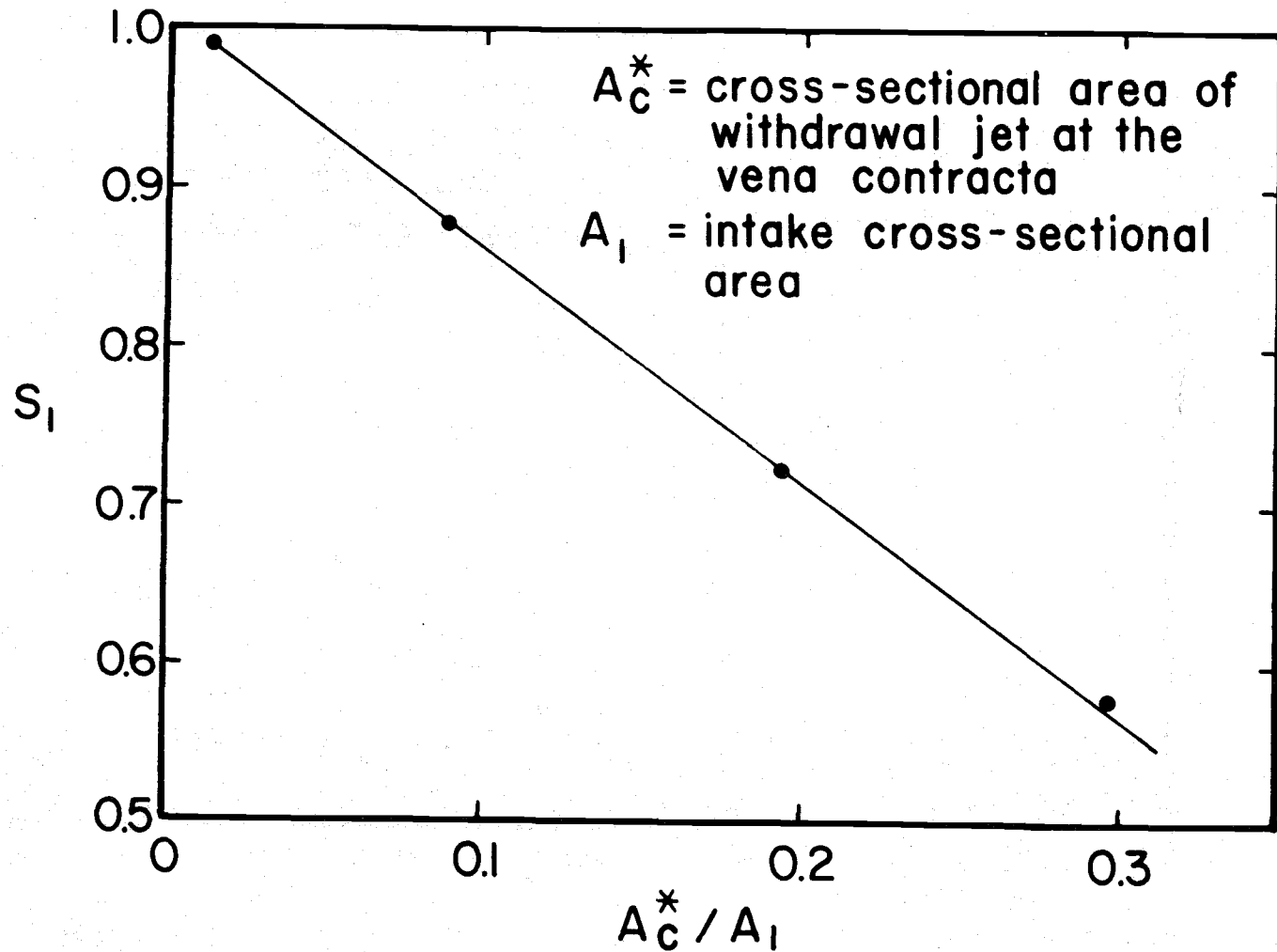
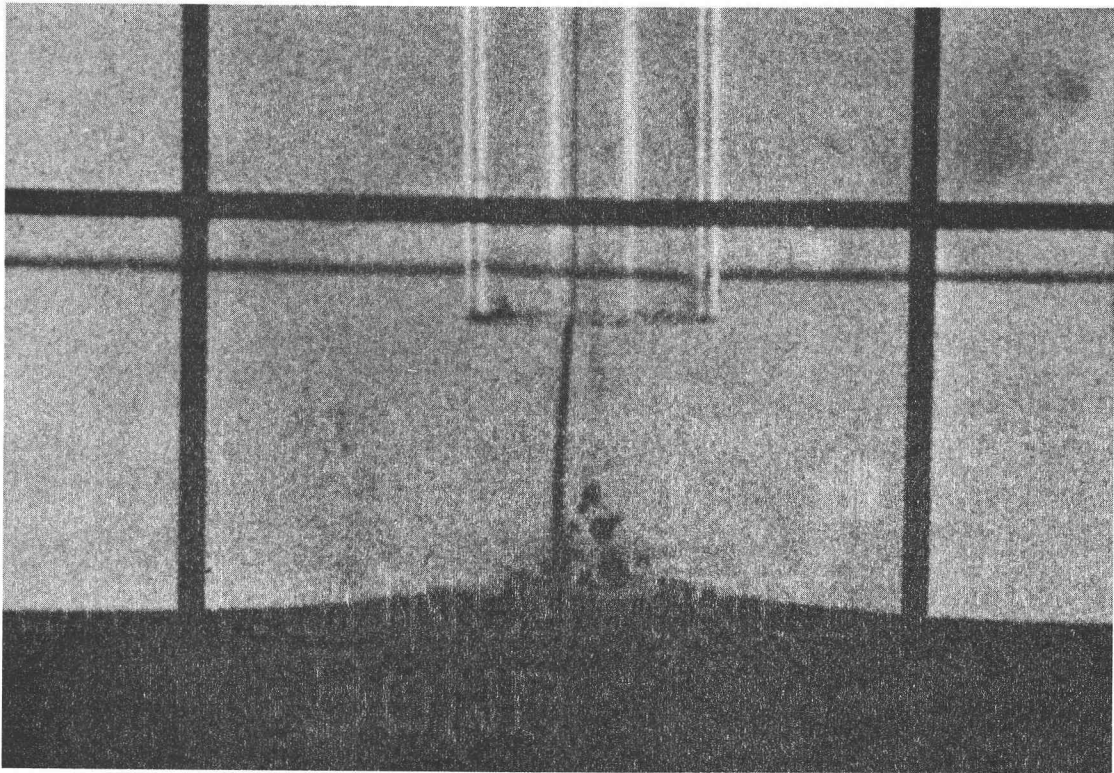


Figure 13. Relation of the degree of selectivity to the cross-sectional area parameter

intake, the mechanism of withdrawal differs from that just discussed. Under these conditions the region immediately beneath the intake is essentially a zone of stagnation with no appreciable fluid motion relative to the intake. The mechanism of withdrawal of the lower layer is due to the presence of the shear region in the immediate vicinity of the density-interface and was observed to be similar to that described by Kuelegan (14). Due to diffusion of the velocity of the upper layer, the upper region of the lower layer is set in motion with the corresponding vertical current. Although the density-interface never reaches the intake, part of the flow from the lower region moves vertically upward into the flowing region of the upper layer and into the intake. This accounts for values of the degree of selectivity less than unity when critical conditions have been exceeded. Picture 2 shows an example of withdrawal under these conditions. Indicator droplets were placed on the interface and were seen to be drawn into the intake while the dyed lower layer was not drawn in. The indicator droplets moved along the density-interface toward the intake under the influence of the shear flow. They were drawn up along the boundary of the stagnant zone which lies immediately below the intake. If the inertial forces were not sufficient to overcome the gravity forces of the spheres, the spheres initially would start up the boundary and then fall into the stagnant zone where they slowly settled back down to the interface. This was clearly observed in the movies from which Picture 2 was taken.

The existence of the shear region may be examined by placing indicator droplet spheres on the density-interface and dropping dye pellets through the layers. The vertical profile of the motion may then



Picture 2. Shear withdrawal from the lower layer:  $\frac{z}{z_c} = 1.19$ ,  
 $\frac{\Delta\rho}{\rho_1} = 0.022$  ,  $u = 0$  ,  $S_1 = 0.96$



be determined, as shown in Figure 14. The velocity of the upper layer increases as it nears the intake while that just below the interface increases and then drops off as it approaches the intake and the stagnation zone. The data for Figure 14 is from a run where  $\frac{\Delta\rho}{\rho_1}$  had a value of 0.022 and the specific test had  $z/z_c = 1.19$  and  $u = 0.0$ .

When linear regression techniques were applied to the data for  $z/z_c$  greater than unity, the simplest expression showing statistical fit was

$$S_1 = 0.916 + 0.038 \left(\frac{z}{z_c}\right), \quad (19)$$

having an  $R^2$  value of 0.252. Extrapolation yields  $z/z_c = 2.24$  for fully-selective withdrawal in terms of the degree of selectivity. Addition of the influence of the density differential across the interface to equation (19) yields

$$S_1 = 0.882 + 0.818\left(\frac{\Delta\rho}{\rho_1}\right) + 0.040\left(\frac{z}{z_c}\right) \quad (20)$$

with an  $R^2$  value of 0.664. Again, an increase in density serves to increase the degree of selectivity of the withdrawal flow. This relationship is shown in Figure 15.

Figure 16 shows regression results of equi-selectivity curves for  $\frac{\Delta\rho}{\rho_1}$  vs.  $\frac{z}{z_c}$ . These curves slope downward to the right and increase in slope with greater values of  $z/z_c$ . One can infer from this that density differences play a minor role when the intake is near the interface but increase in importance as the separating distance increases. The regression results were obtained from data with  $z/z_c$  less than 1.1. The resulting equation is

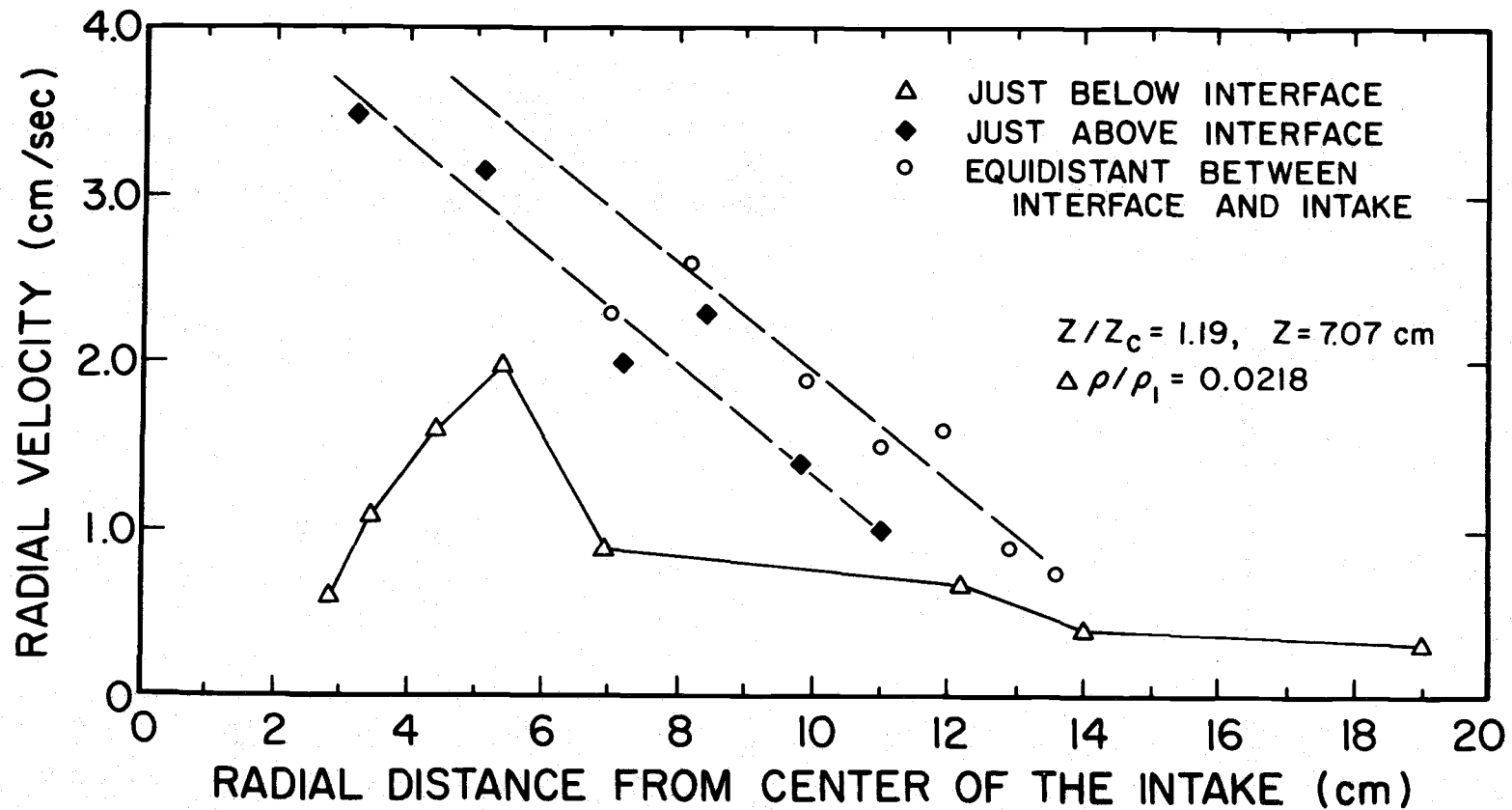


Figure 14. Relation of the radial velocity to the radial distance from the intake

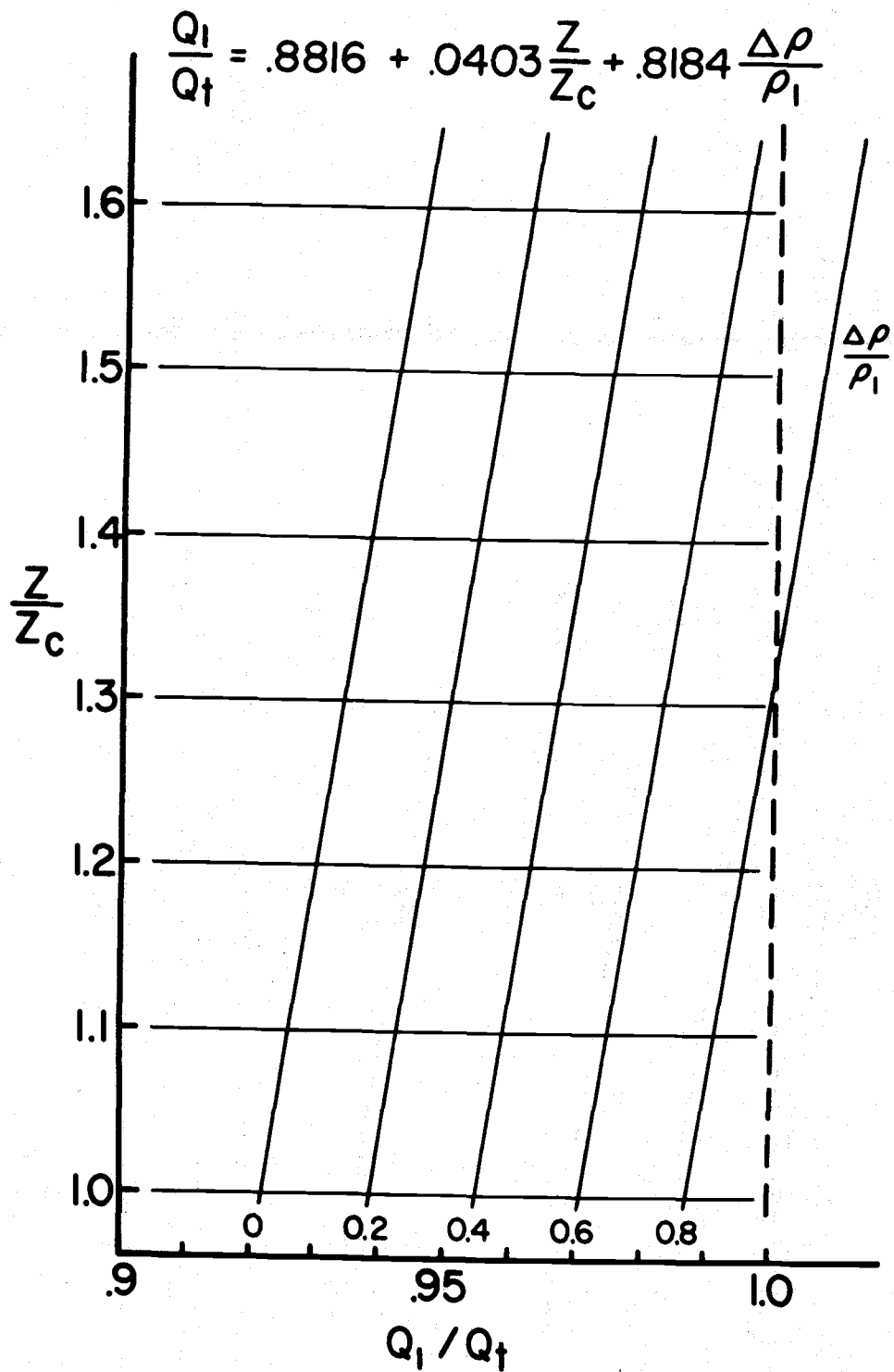


Figure 15. Influence of the density differential on the degree of selectivity; proximity parameter greater than unity

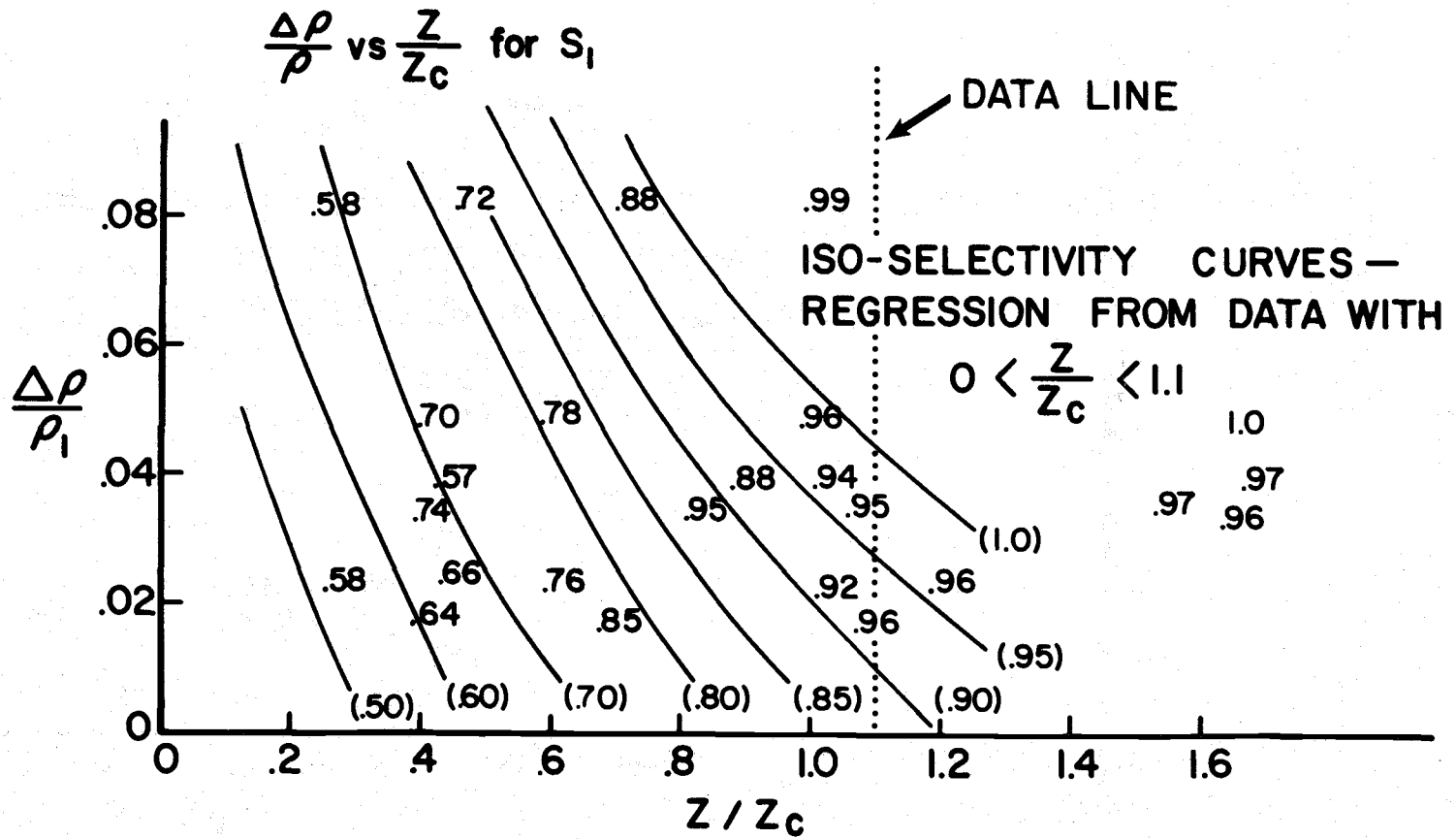


Figure 16. Iso-selectivity curves

$$\frac{\Delta\rho}{\rho_1} = -0.089 + 0.335 S_1 - 0.253 \tanh\left(\frac{z}{z_c}\right) \quad (21)$$

for which an  $R^2$  value of 0.205 is obtained. While the general fit is not the best, the suggested trends appear to be valid. Within the range of data,  $1.0 < z/z_c < 1.7$ , the density difference is more important than the value of  $z/z_c$ . When regression techniques were applied to obtain equation (19) the first variable to enter was  $\frac{\Delta\rho}{\rho_1}$ , giving the expression

$$S_1 = 0.934 + 0.781 \frac{\Delta\rho}{\rho_1} \quad (22)$$

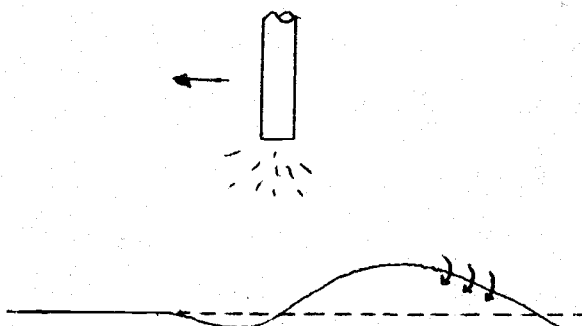
for which an  $R^2$  value of 0.377 was obtained; as compared to the  $R^2$  value of 0.252 for equation (19).

#### Influence of an Ambient Current

A group of tests with various speeds of towing of the intake were run as part of the experiment to simulate ambient currents in proximity to the selective withdrawal intake. All tests in a series were made with approximately the same value of the proximity parameter. In most tests the discharge through the pump was sampled to obtain a specimen for determining the withdrawal degree of selectivity; also, movies were taken of the flow field. Thus any observable motion could be quantified and if possible, correlated with the degree of selectivity.

The formation of waves on the density-interface was examined as a function of the towing speed of the intake. In some of these laboratory tests the lower layer was dyed, though the layers were easily distinguish-

able by the index of refraction. Indicator droplets were placed on the interface along the path of the intake so that incipient motion could easily be photographed. The results show that the wave phenomenon is dependent, among other things, on whether or not a withdrawal cone is present (the critical condition of the proximity parameter). Series of tests with  $z$  greater than  $z_c$  indicated that at low towing velocities no waves were formed on the density-interface. The indicator droplets directly under the intake (within the stagnation zone) showed a tendency to move along with the intake, but eventually fell behind. At moderate velocities a small amplitude wave was observed on the density-interface with its crest moving at the same velocity as the intake and in the same direction. The crest remained slightly ahead of the center-line of the intake. In some runs, by the time the intake structure reached the end of the tow a second wave appeared to possibly be forming ahead of the first, indicating the group velocity of the waves which were formed was greater than the velocity of the intake. At greater relative velocities a wave of larger amplitude was generated. The wave crest moved at the same velocity as the intake but was located behind the intake. From the motion of the indicator droplets it appears that the wave crest spilled backwards as it moved, as sketched below. Accordingly a wave train was



left behind the moving intake.

When the value of  $z$  was less than critical and a withdrawal cone was present the density-interface was more resistant to wave formation. At a low velocity no waves were formed (less than 1.2 cm/sec. for these tests). The indicator droplets, both upstream and downstream from the intake, had velocities exceeding that of the intake; and spheres located downstream from the intake were eventually drawn in. At greater relative velocities waves were formed but they were of small amplitude. The only region of appreciable mixing appeared to be in the vicinity immediately following the intake. Figure 17 shows the typical locations and shapes of the withdrawal cones at relative velocities of 1.25, 5.76, and 10.25 centimeters per second. These were resolved from a run which had the lower layer dyed so that the position of the withdrawal cone could be observed at various relative velocities. The shaded region on the back side of the cone in Figure 17 - a represents an area where the dye interface was not distinct. This region had an apparently high degree of shear mixing. In Figure 17 - c the interfacial region immediately behind the intake was unstable (showing short-lived patches of turbulence).

The degree of selectivity of the withdrawal flow, in the presence of an ambient current, was found to depend on the formation and location of waves on the density-interface., as well as on the other parameters discussed ( $z/z_c$ , density differential parameter, etc.). The selectivity of the flow increased with low relative velocities and the absence of waves. Then, as waves were formed, the selectivity appeared to depend on the location of the crest or cone, relative to the intake. With the crest below the intake the selectivity of the withdrawal decreased, and reached

## INTAKE MOVING TO THE LEFT

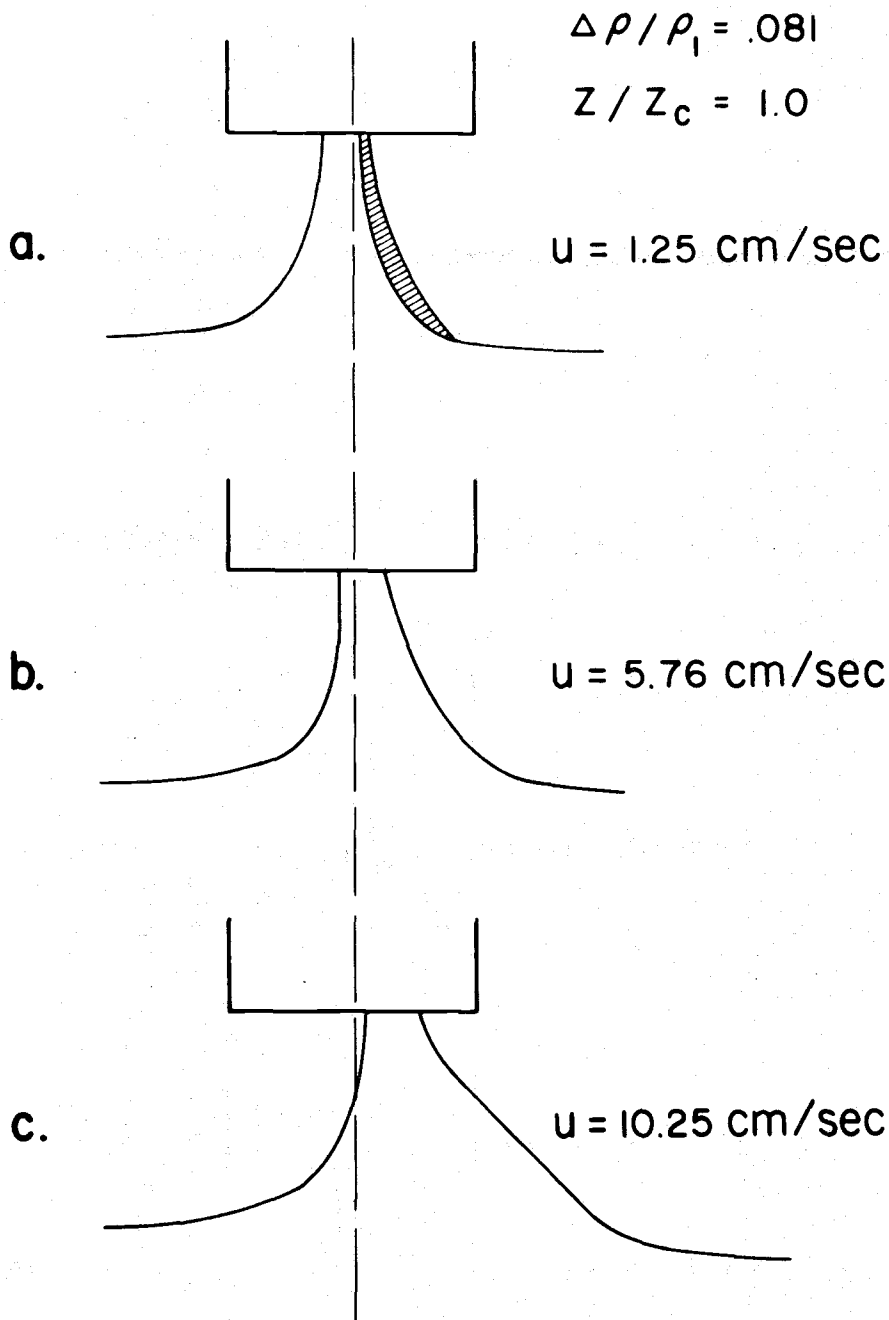


Figure 17. Typical locations and shapes of withdrawal cones



a minimum with moderate relative velocities. For relative velocities greater than this the wave crest was far enough behind the intake so it had little influence on the withdrawal flow and the degree of selectivity increased. If such interfacial waves can be excluded, then an ambient current would be expected to allow the intake to draw more strongly from its own level of immersion.

The relationship between selectivity and the magnitude of the ambient current may be examined in terms of increases and decreases in the measured degree of selectivity relative to that expected under identical withdrawal conditions but with no ambient current. By plotting this relative selectivity ratio against the intake velocity, the response of the 'measured' selectivity is seen relative to the 'expected' selectivity under identical conditions but with zero ambient current. Values greater than unity indicate the withdrawal flow is more selective than the corresponding stagnant case, and thus suggest that the relative velocity serves to enhance the withdrawal phenomena.

Figure 18 - A shows the relation between the selectivity ratio and the tow velocity for values of the density differential and proximity parameters of about 0.045 and 0.6, respectively. The range of the relative selectivity falls between 0.92 and 1.12, for the series shown, which corresponds to a measured degree of selectivity falling between 0.73 and 0.88. If this is reduced still further, the range of the ratio of the discharge from the upper and lower layers ( $Q_1:Q_2$ ) is 950:350 at a towing speed of 8.3 centimeters per second and 1150:150 at 21.5 centimeters per second (with  $Q_t$  equal to 1300 cubic centimeters). The magnitude of the change in discharge ratio for changes in the velocity of towing

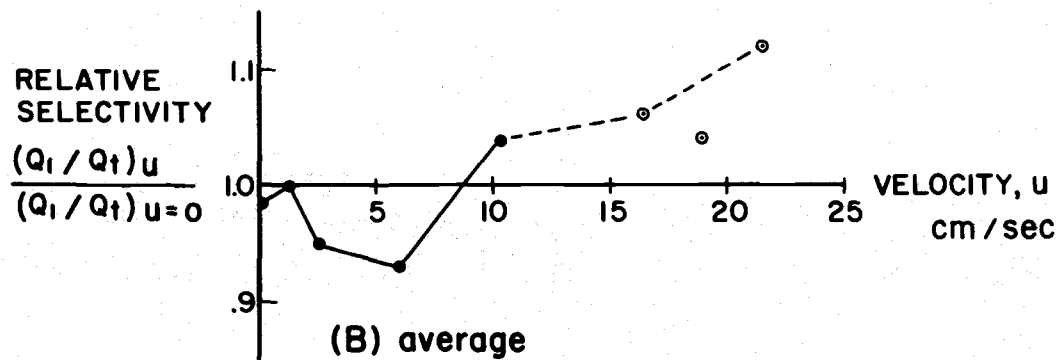
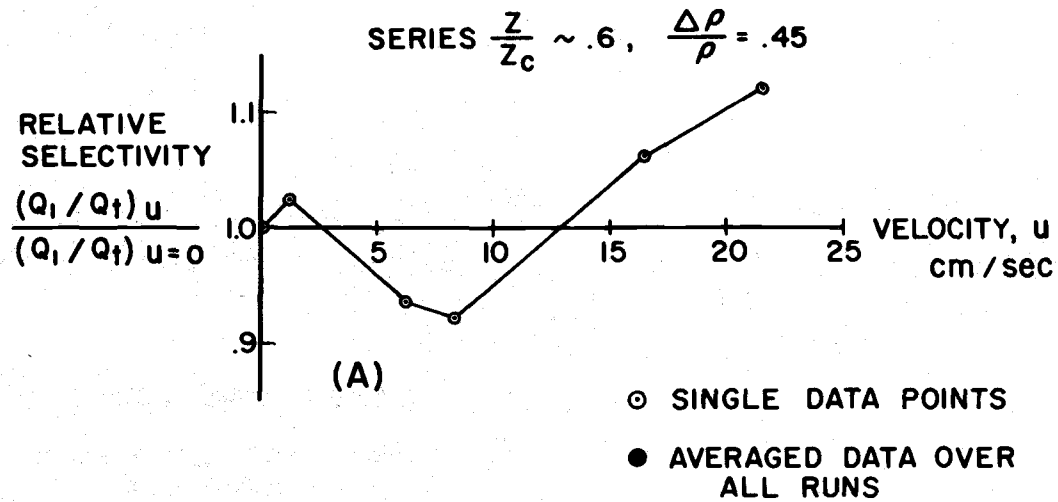


Figure 18. Relation of the relative selectivity to the ambient velocity

increases for smaller values of the proximity parameter and decreases for larger values.

Figure 18-(B) shows the averaged response for various ranges of  $z/z_c$ , taken over all series of all runs. The regions showing decreases in selectivity corresponded well with observed large amplitude waves in the immediate vicinity of the intake as seen in films of the tests. Increases in intake velocity resulted in having these waves located further behind the intake, and thus having less of an effect on the withdrawal flow. This situation corresponds to the increases in selectivity at high velocities.

Figure 19 shows a similar relationship for two series, both having  $\Delta\rho$  values of 0.022. Figure 19-(a) shows the relationship between the ratio of the measured degree of selectivity to the degree of selectivity calculated from equation (18) and the magnitude of the simulated ambient current. The proximity parameter has a value of about 0.6. Figure 19-(b) shows the same type of relationship for a  $z/z_c$  value of 1.20. In this case the expected degree of selectivity was calculated from equation (20). The similarity in the two graphs is apparent.

A number of interesting phenomena related to the moving intake and the withdrawal cone were noted. If the withdrawal flow is started and increased slowly until the desired discharge is reached, the cone which is formed approaches its equilibrium shape and size asymptotically. If the intake is stationary, the shape and size of the withdrawal jet remains constant. In contrast to this, if the withdrawal flow is started and immediately brought to its final discharge level the withdrawal jet overshoots its equilibrium size and oscillates about the equilibrium condition

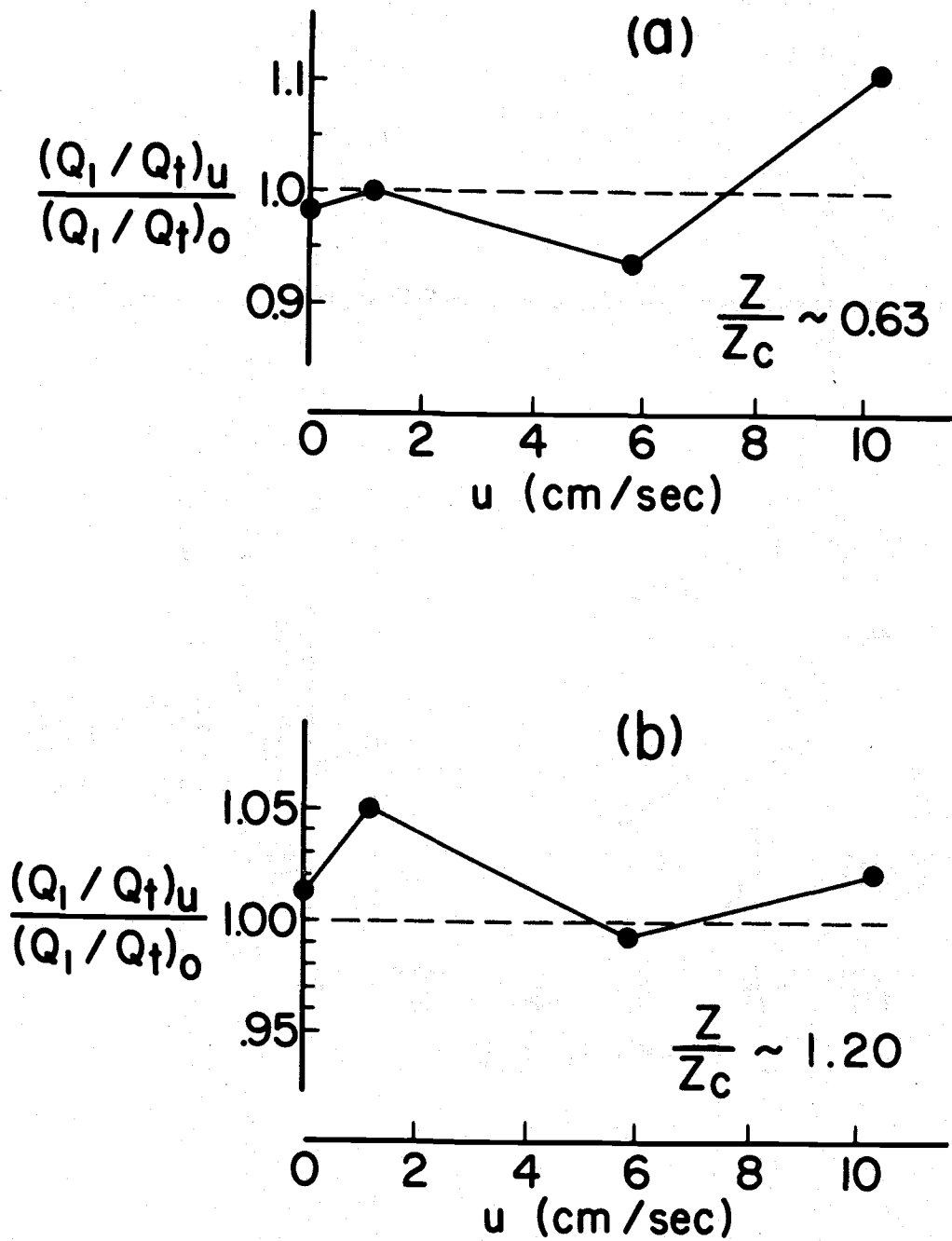


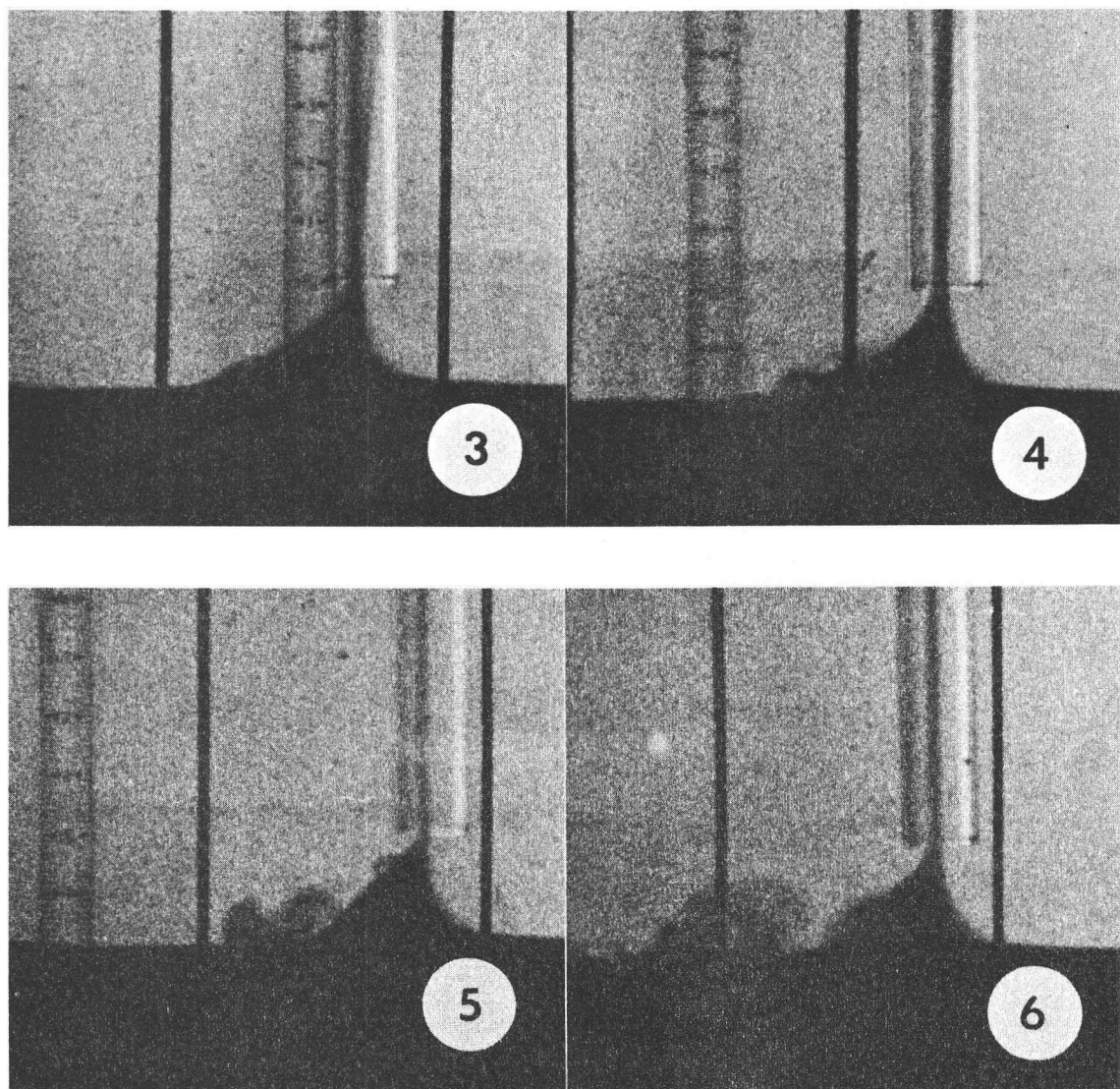
Figure 19. Relation of the relative selectivity to the ambient velocity;  
 $\frac{\Delta\rho}{\rho_1} = 0.022$

(which is a function of gravity, inertial, and viscous forces). The selectivity of the withdrawal flow appears to fluctuate with the pulsations of the withdrawal cone; first drawing greater amounts from the lower layer and then less, and so on.

The pulsation motion is similar in nature to the relaxation of streamlines of the flow into a line sink located at the bottom boundary in a stratified flow field; as discussed by Kao, Pao, and Wei (13). In their study, unsteady flow of a stratified fluid was started from rest and the streamline behavior subsequently observed. These streamlines relax and with increasing time approach the sink at less of an angle with the bottom boundary. At even later times, blocking of the fluid immediately above the intake was observed.

In the present case the pulsations became damped out. The pulsations are quite noticeable at high values of  $z/z_c$  (but still less than unity) while at low values, when the intake was close to the density-interface, the pulsations were not observed or were damped immediately. This type of motion was also present when the cone moved with the intake. Under these conditions the pulsations served to make the cone unstable to capillary sheading.

Capillary sheading was the only observed mode of instability of the density-interface; and was confined to the region immediately behind the moving intake. No instabilities were observed when the intake was held stationary. Instabilities are due to the shear velocity associated with the interfacial region; capillary waves gain too much energy and a sheet lifts off the density-interface into the upper layer. Such a sequence of capillary entrainment is shown in Pictures 3 - 6.



Pictures 3-6. Capillary entrainment sequence where  $u = 10.3$  cm/sec.

In examining the nature of the flow at the intake, the results given in Figures 12 and 13 are further analysed. Since the withdrawal jet is symmetrical with respect to the axis of the intake, the cross sections of the flow at the mouth of the intake and at the vena contracta are expected to project as two concentric circles. The inner circle contains the flow from the lower layer while the outer flow region contains the flow from the upper layer. With the diameters for the two locations given in Figure 12, the cross-sectional areas may be calculated. Knowledge of the degree of selectivity allows calculation of the discharges from each layer. With this information the mean velocities of the two areas could be determined. Knowledge of the cross-sectional areas at the intake mouth and the vena contracta allows calculation of an intake choking coefficient for the two-layer withdrawal flow, as a function of  $z/z_c$ . This is shown in Figure 20.

#### Significance for Thermocline Structure

The results of this study may be relevant to discussions on the stability of a thermocline in the vicinity of a withdrawal intake. Woods (25) and Woods and Fosberry (26) have discussed the structure of the thermocline in the sea as composed of alternating sheets having great temperature or density gradients and strong localized shear, and layers having much greater widths and much weaker static stability and shear. A feature of the sheets are long coherent trains of steep internal gravity waves. The strong shear at the crest of these waves has been observed to give Kelvin-Helmholtz instability. Woods has suggested that heat is

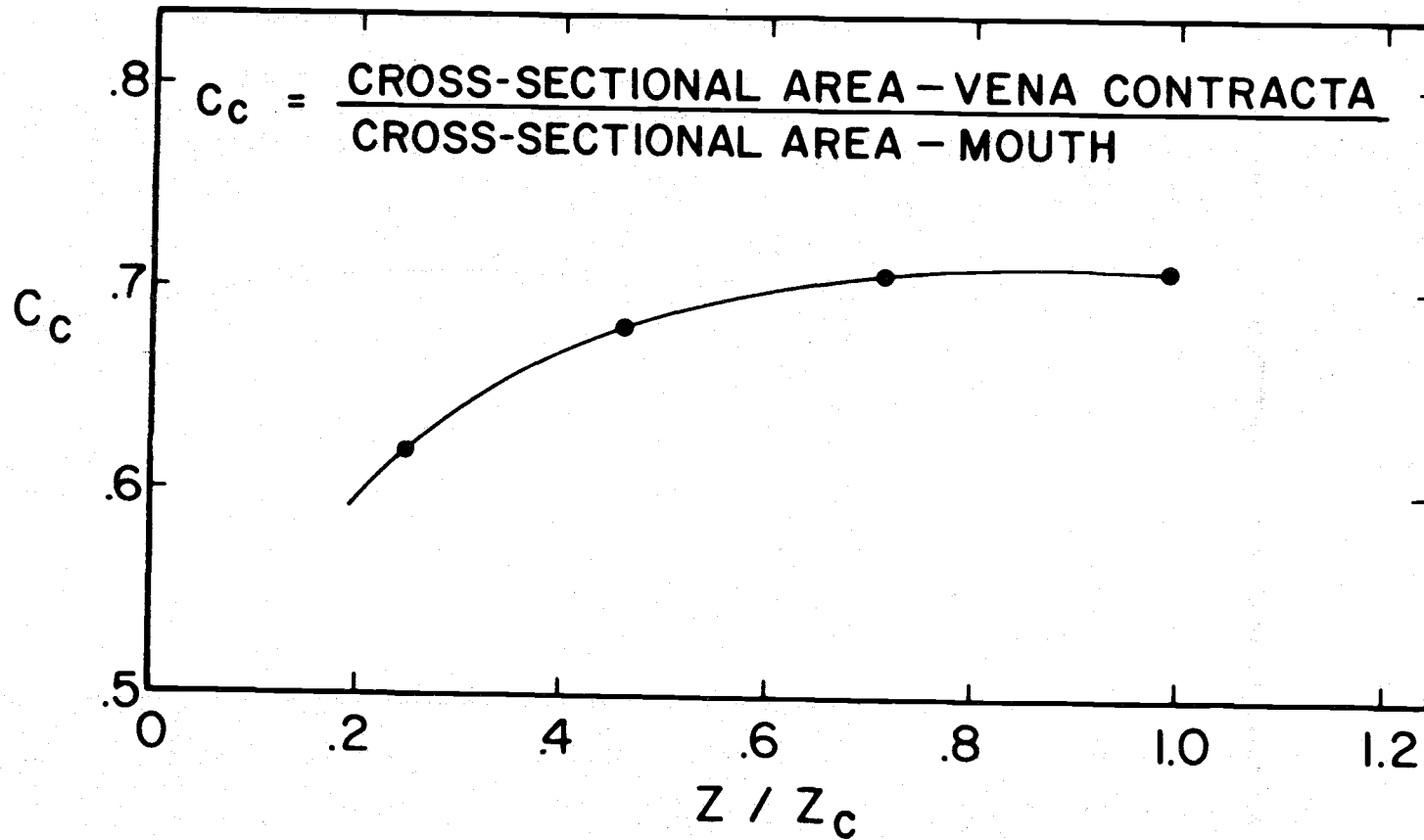


Figure 20. Relation of the choking coefficient to the proximity parameter



able to penetrate the sheets spasmodically during the formation and decay of breaking waves (and the short lived patch of turbulence they produce). If this is the case, the presence of internal waves may influence the temperature difference across a given sheet and the subsequent structure of the thermocline.

In the presence of a withdrawal current, waves may be generated within these sheets as they are advected past the intake structure; it is expected that the generated waves will have a large amplitude even when the thermocline is not within the boundary of the withdrawal flow. The number of breaking internal waves might increase, allowing for an increase in heat flux and subsequent decrease in stability. Thus, to insure the persistence of the thermocline structure and its stability, in the presence of an ambient current, withdrawal intakes must be located at increased depths below the thermocline than those suggested by previous investigations of the selective withdrawal phenomenon.

## V. CONCLUSIONS

The behavior of flow withdrawal into a vertically suspended upper strata point sink was examined experimentally to investigate the influence of an ambient current. Selectivity was defined as the bias of withdrawing one layer more strongly than the other, the degree of selectivity being a measure of the magnitude of the bias. Tests were made for various density differentials across the interface, elevations between the intake and the interface, and relative velocities between the flow field and the intake.

The results of this study show that the presence of an ambient current will influence the selectivity of the withdrawal flow; the general trend being for the current to enhance the selectivity as the magnitude of the current increases. This trend is partially masked by the formation of interfacial waves at moderate velocities of the current, or in the present study, of the towed intake structure. When the crest of generated waves remain in the immediate vicinity of the intake the withdrawal selectivity decreases. As the current increases and the wave crest falls further behind the intake the selectivity increases. At high ambient currents the selectivity of the withdrawal flow is expected to be greatly enhanced, though the interfacial region behind the intake will probably be greatly disturbed. The effect of an ambient current is to allow the intake to draw more strongly from its own level of immersion. The generation of interfacial waves may be a more important consequence of an ambient current than its influence on the degree of selectivity; especially as the interfacial waves relate to the subsequent structure

of the flow field.

The results also show that within a range of separating heights of the intake from the interface, the degree of selectivity approaches the value of unity slowly after passing a critical value of the separating height. The influence of the density difference across the interfacial region is negligible when the intake is close to the density-interface, but increases in importance as the separating height is increased.

## BIBLIOGRAPHY

1. Abraham, G., Some aspects of surface water wave scale effects, Proceedings, ASCE, Vol. 87, No. HY 1, January, 1961.
2. Batchelor, G. K., Introduction to Fluid Dynamics, Cambridge University Press, London, England, 1970.
3. Brooks, N.H. and Koh, R.C.Y., Selective withdrawal from density-stratified reservoirs, Proceedings, ASCE, Vol. 95, No. HY 4, July, 1969.
4. Craya, A., Theoretical research on the flow of nonhomogeneous fluids, La Houille Blanche, 4, 1949.
5. Debler, W.R., Stratified flow into a line sink, Proceedings, ASCE, Vol. 85, No. EM 3, July, 1959.
6. Gariel, P., Experimental research on the flow of nonhomogeneous fluids, La Houille Blanche, 4, 1949.
7. Harleman, D.R.F., Morgan, R.L., and Purple, R.A., Selective withdrawal from a vertically stratified fluid, 8th Congress, International Association for Hydraulic Research, August, 1959.
8. Harleman, D.R.F., Stratified flow, Handbook of Fluid Dynamics (ed. Streeter), Chapter 26, McGraw-Hill, 1961.
9. Huber, D.G., Irrotational motion of two fluid strata towards a line sink, Proceedings, ASCE, Vol. 86, No. EM 4, August, 1960.
10. Huber, D.G. and Reid, T.L., Experimental study of two-layered flow through a sink, Proceedings, ASCE, Vol. 92, No. HY 1, January, 1966.
11. Industrial Waste Guide on Thermal Pollution, U.S. Department of the Interior, Federal Water Pollution Control Administration, Corvallis, Oregon, September, 1968.
12. Kao, T.W., A free-streamline solution for stratified flow into a line sink, J. Fluid Mechanics, Vol. 21, part 3, 1965.
13. Kao, T.W., Pao, H.P., and Wei, S.N., Time-dependent behavior of stratified flow in a channel toward a line sink, International Symposium on Stratified Flows, 1973.
14. Keulegan, G.H., Laminar flow at the interface of two liquids, J. Research of the National Bureau of Standards, Vol. 32, Research Paper RP1591, June, 1944.

15. Koh, R.C.Y., Viscous stratified flow towards a sink, J. Fluid Mechanics, Vol. 24, part 3, 1966.
16. Lamb, H., Hydrodynamics, 6th Edition, Dover Publications, New York, New York, 1945.
17. Long, R.R., Velocity concentrations in stratified fluids, J. Hydraulics Division, ASCE, Vol. 88, part 1, January, 1962.
18. Lubin, B.T. and Springer, G.S., The formation of a dip on the surface of a liquid draining from a tank, J. Fluid Mechanics, Vol. 29, part 2, 1967.
19. Rouse, H., Seven exploratory studies in hydraulics, Proceedings, ASCE, Vol. 82, No. HY 4, August, 1956.
20. Rumer, R.R., Interfacial wave breaking in stratified liquids, Proceedings, ASCE, Vol. 99, No. HY 3, March, 1973.
21. Wiegel, R.L., Snyder, C.M., and Williams, J.E., Water gravity waves generated by a moving low pressure area, Transactions, American Geophysical Union, Vol. 39, No. 2, April, 1958.
22. Williams, J.M., A practical assessment of selective withdrawal, From correspondence with L.S. Slotta following the Symposium on Mathematical and Hydraulic Modeling of Estuarine Pollution, April, 1972.
23. Woods, J.D., Micro-oceanography, Underwater Science (ed. Woods and Lythgoe), Chapter 9, Oxford University Press, 1971.
24. Woods, J.D. and Fosberry, G.G., The structure of the thermocline, Underwater Association Report, 1966-67.
25. Yih, C.S., On the flow of a stratified fluid, Proceedings, 3rd U. S. National Congress of Applied Mechanics, 1958.
26. Yih, C.S., Dynamics of Nonhomogeneous Fluids, Chapter 3, MacMillan Co., New York, N.Y., 1965.

## APPENDIX

Test Data:  $D = 3.175 \text{ cm}$  ,  $Q_t = 1300 \text{ cm}^3/\text{sec}$

$u$ (cm/sec)	$z$ (cm)	$\frac{z}{z_c}$	$S_1 = \frac{Q_1}{Q_t}$	$\frac{\Delta\rho}{\rho_1}$	$h_1$ (cm)	$h_2$ (cm)
0	8.14	1.54	0.97	0.0344		
1.25	8.14	1.54	0.98	0.0344		
6.25	8.14	1.54	0.98	0.0344		
0	5.61	1.06	0.95	0.0344		
1.25	5.61	1.06	0.98	0.0344		
6.25	5.61	1.06	0.96	0.0344		
0	6.06	1.01	0.92	0.0209		
1.25	6.16	1.03	1.00	0.0209		
6.25	6.31	1.05	0.98	0.0209		
0	8.81	1.64	0.96	0.0333	31	14
1.25	8.81	1.64	1.00	0.0333	29	14
6.25	8.81	1.64	0.98	0.0333	27	14
0	4.42	0.82	0.95	0.0333	26	14
1.25	4.42	0.82	0.96	0.0333	25	14
6.25	4.42	0.82	0.94	0.0333	23	14
0	2.13	0.40	0.74	0.0333	22	14
1.25	2.13	0.40	0.76	0.0333	21	14
6.25	2.13	0.40	0.71	0.0333	19	13
0	6.89	1.07	0.96	0.0160	31.2	14.2
2.44	6.89	1.07	0.95	0.0160	29.4	14.2
10.32	6.89	1.07	0.89	0.0160	27.9	14.2
0	4.51	0.70	0.85	0.0160	26.6	14.0
2.44	4.75	0.74	0.81	0.0160	24.6	13.7
10.32	5.05	0.79	0.94	0.0160	22.3	13.4
5.76	5.05	0.79	0.77	0.0160	20.9	13.4
0	2.50	0.39	0.64	0.0160	19.6	13.2
0.80	2.86	0.44	0.66	0.0160	18.1	12.9
1.20	2.86	0.44	0.68	0.0160	16.4	12.5
2.44	3.20	0.50	0.67	0.0160	14.7	12.2
5.76	2.77	0.43	0.63	0.0160	13.2	11.8
10.32	3.05	0.48	0.66	0.0160	12.0	11.6
0	4.23	0.99	0.99	0.0811	25.3	14.4
1.20	4.27	1.00	0.98	0.0811	24.1	14.3
5.76	4.30	1.01	0.96	0.0811	22.7	14.3
10.32	4.30	1.01	0.95	0.0811	22.0	14.3
0	3.02	0.71	0.88	0.0811	20.1	14.2
0	1.95	0.46	0.72	0.0811	19.2	14.2
0	1.07	0.25	0.58	0.0811	18.0	14.0

Test Data (cont):  $D = 3.175 \text{ cm}$  ,  $Q_t = 1300 \text{ cm}^3/\text{sec}$

$u$ (cm/sec)	$z$ (cm)	$\frac{z}{z_c}$	$S_1 = \frac{Q_1}{Q_t}$	$\frac{\Delta\rho}{\rho_1}$	$h_1$ (cm)	$h_2$ (cm)
0	7.07	1.19	0.96	0.0218	31.1	14.3
1.20	7.07	1.19	1.00	0.0218	29.5	14.3
5.76	7.16	1.20	0.94	0.0218	25.9	14.2
5.76	7.07	1.19	0.94	0.0218	26.5	14.3
5.76	7.07	1.19	0.97	0.0218	28.1	14.3
10.32	7.19	1.21	0.97	0.0218	24.9	14.2
0	3.53	0.59	0.76	0.0218	21.7	14.0
1.20	3.81	0.64	0.80	0.0218	20.8	13.7
5.76	3.96	0.67	0.76	0.0218	19.2	13.5
10.32	3.93	0.66	0.97	0.0218	18.4	13.3
10.32	4.14	0.70	0.84	0.0218	17.1	13.1
0	2.68	0.45	0.66	0.0218	16.3	13.0
0	1.52	0.26	0.58	0.0218	15.2	12.7

Test Data:  $D = 2.54 \text{ cm}$  ,  $Q_t = 1220 \text{ cm}^3/\text{sec}$

$u$	$z$	$\frac{z}{z_c}$	$S_1$	$\frac{\Delta\rho}{\rho_1}$
0	8.43	1.54	0.98	0.0351
1.20	8.43	1.54	0.98	0.0351
2.44	8.43	1.54	0.97	0.0351
0	5.94	1.09	0.98	0.0351
0	3.68	0.68	0.83	0.0351
0	2.38	0.44	0.68	0.0351
0	4.84	0.94	0.98	0.0423
6.13	4.87	0.94	0.96	0.0423
18.80	5.00	0.97	1.00	0.0423
0	2.99	0.58	0.78	0.0423
8.31	3.23	0.62	0.74	0.0423
16.40	3.47	0.67	0.88	0.0423
21.50	2.71	0.52	0.84	0.0423